

# Medial Representations

## Mathematics, Algorithms and Applications

Kaleem Siddiqi

School of Computer Science & Centre For Intelligent Machines

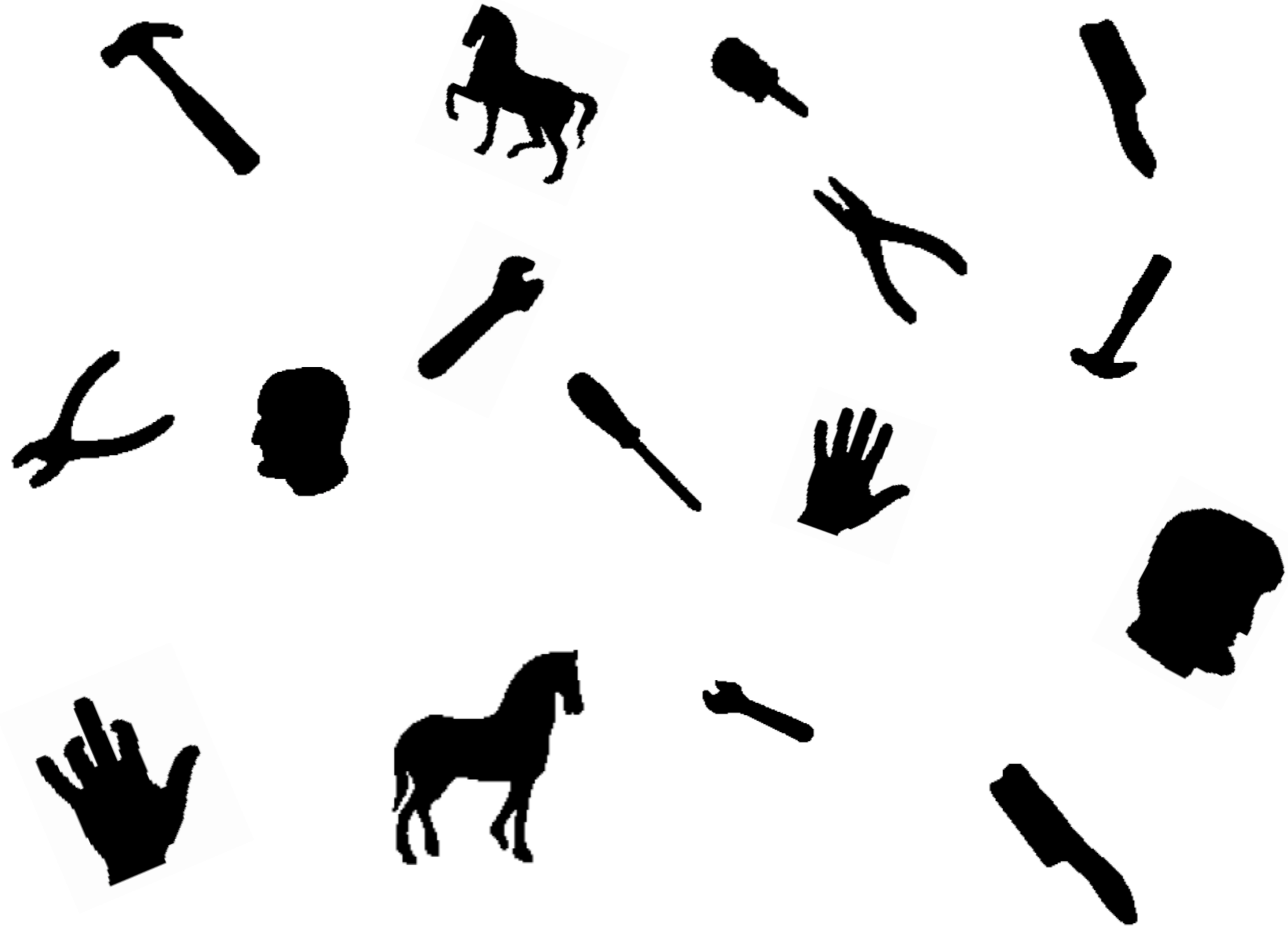
McGill University

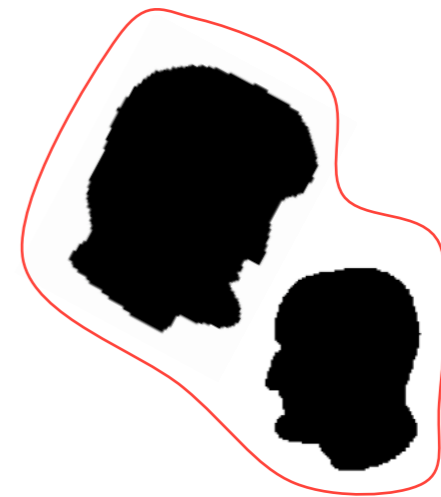
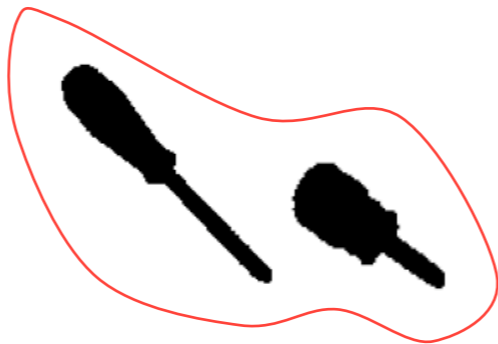
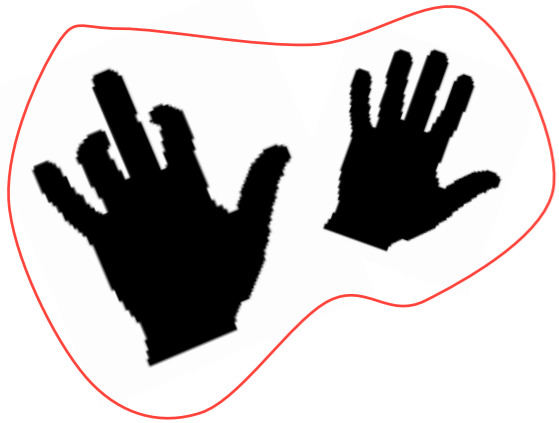
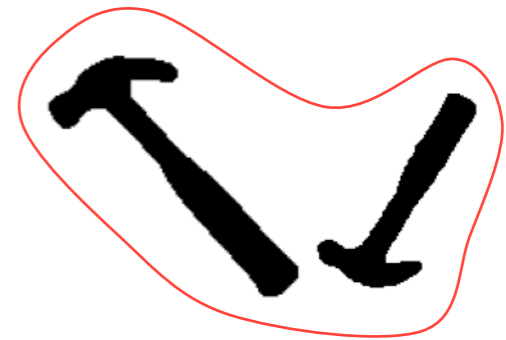
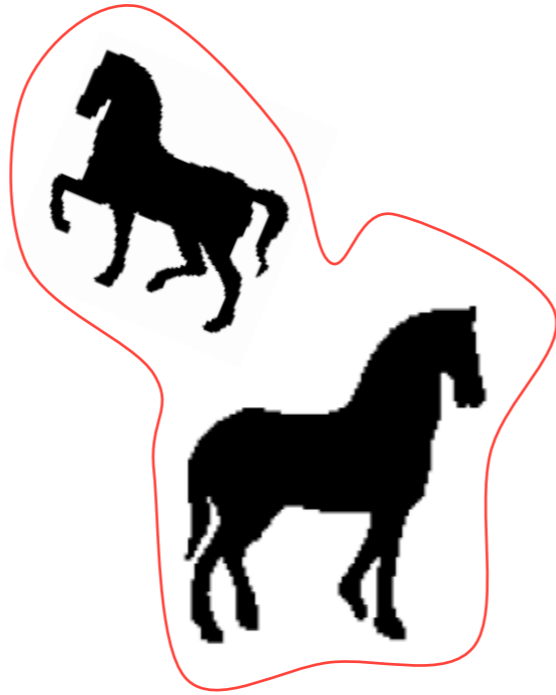
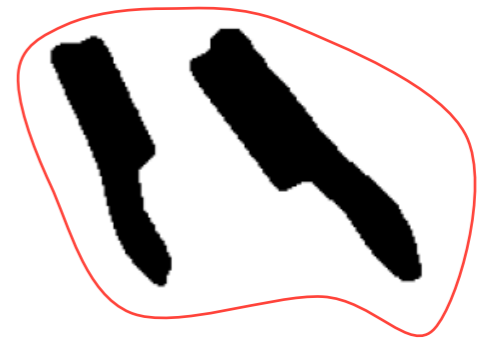
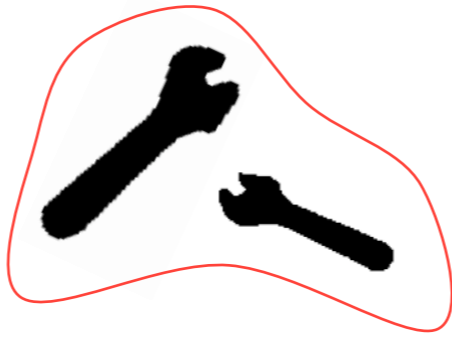
<http://www.cim.mcgill.ca/~shape>

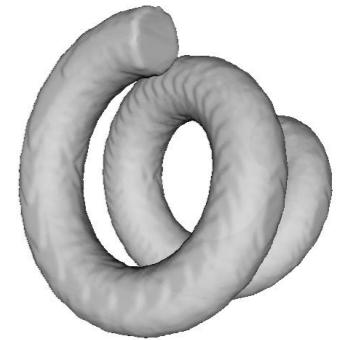
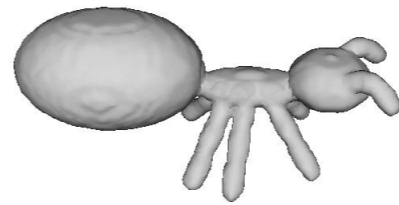
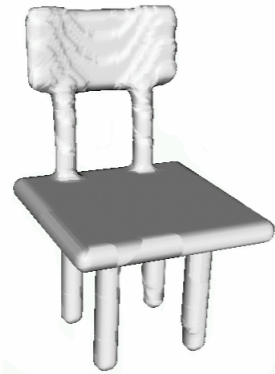
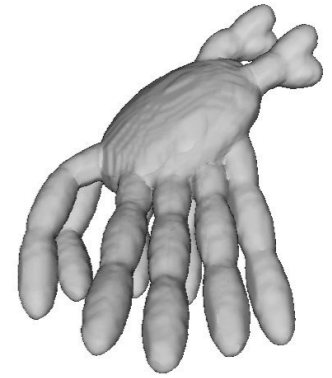
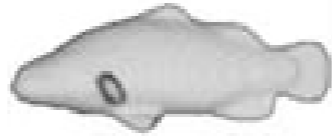
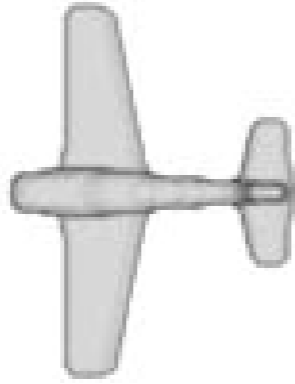
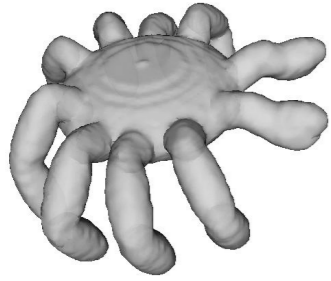
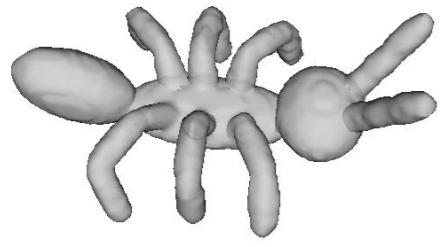
with contributions from:

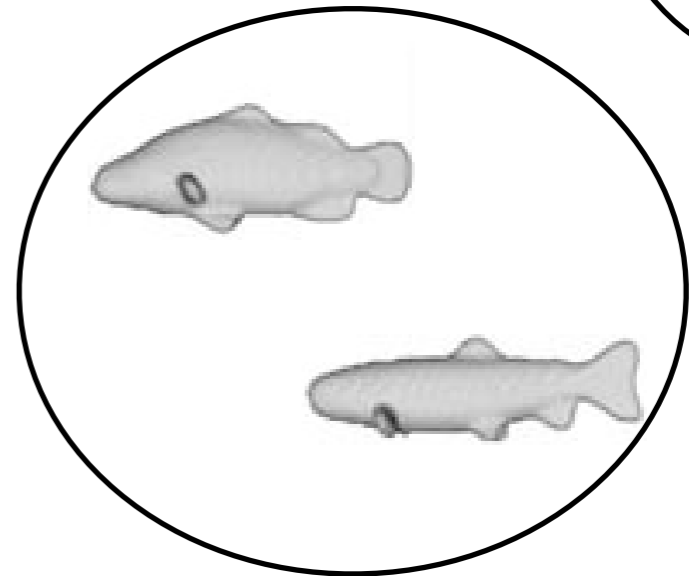
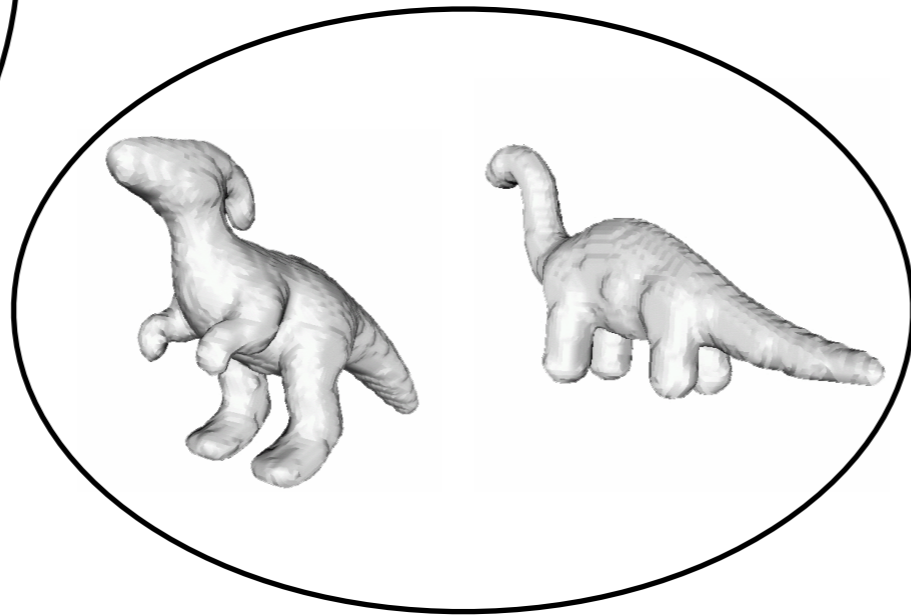
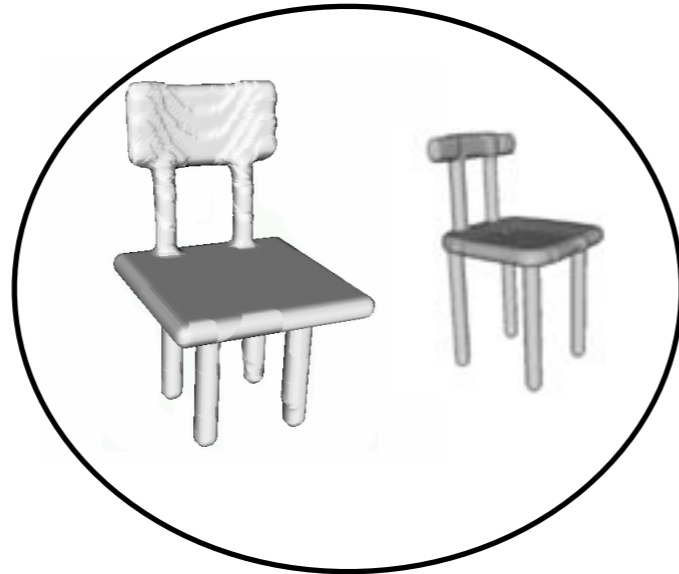
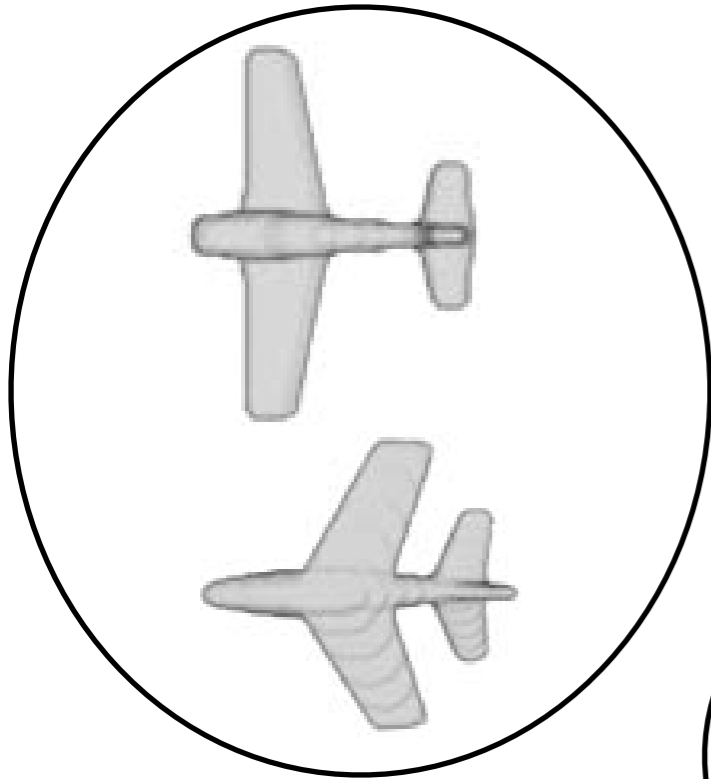
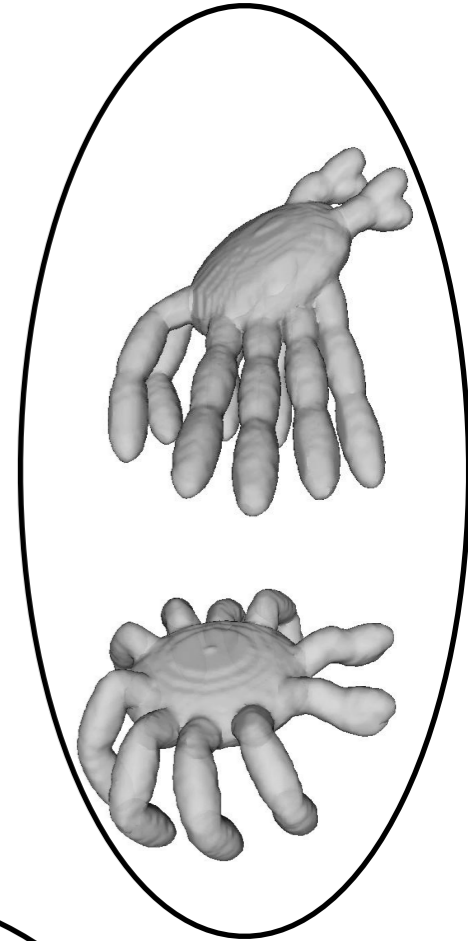
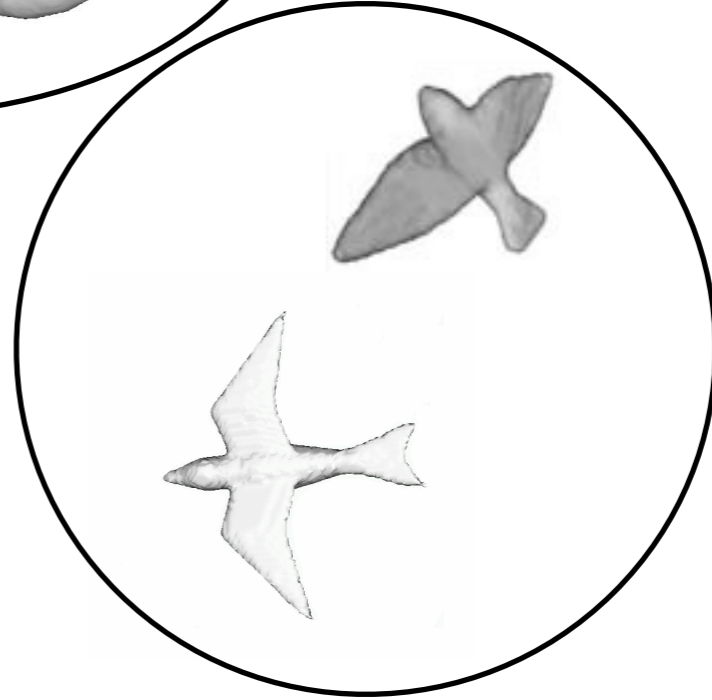
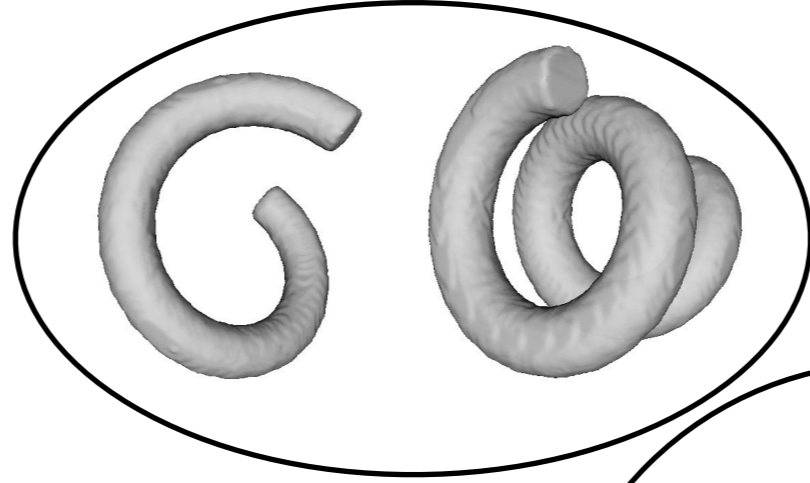
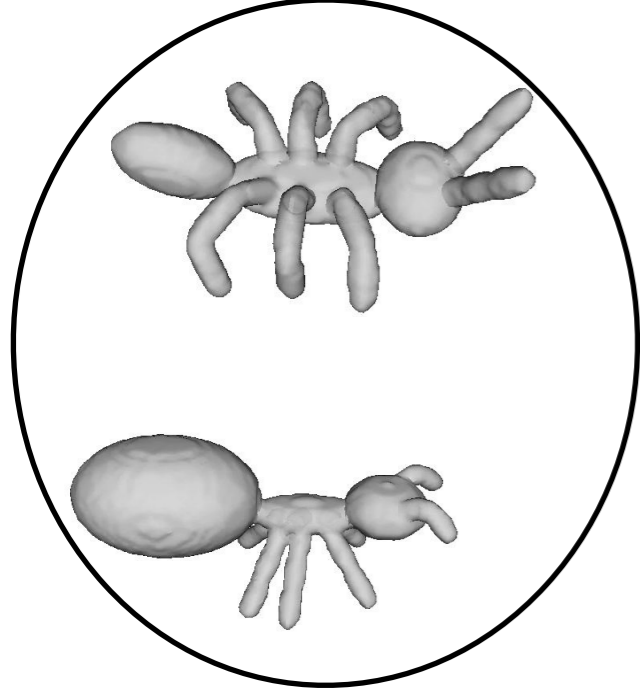
Sylvain Bouix, James Damon, Sven Dickinson, Pavel Dimitrov, Diego Macrini,  
Marcello Pelillo, Carlos Phillips, Ali Shokoufandeh, Svetlana Stolpner, Steve Zucker,

Motivation









# Blum's A-Morphologies: 2D

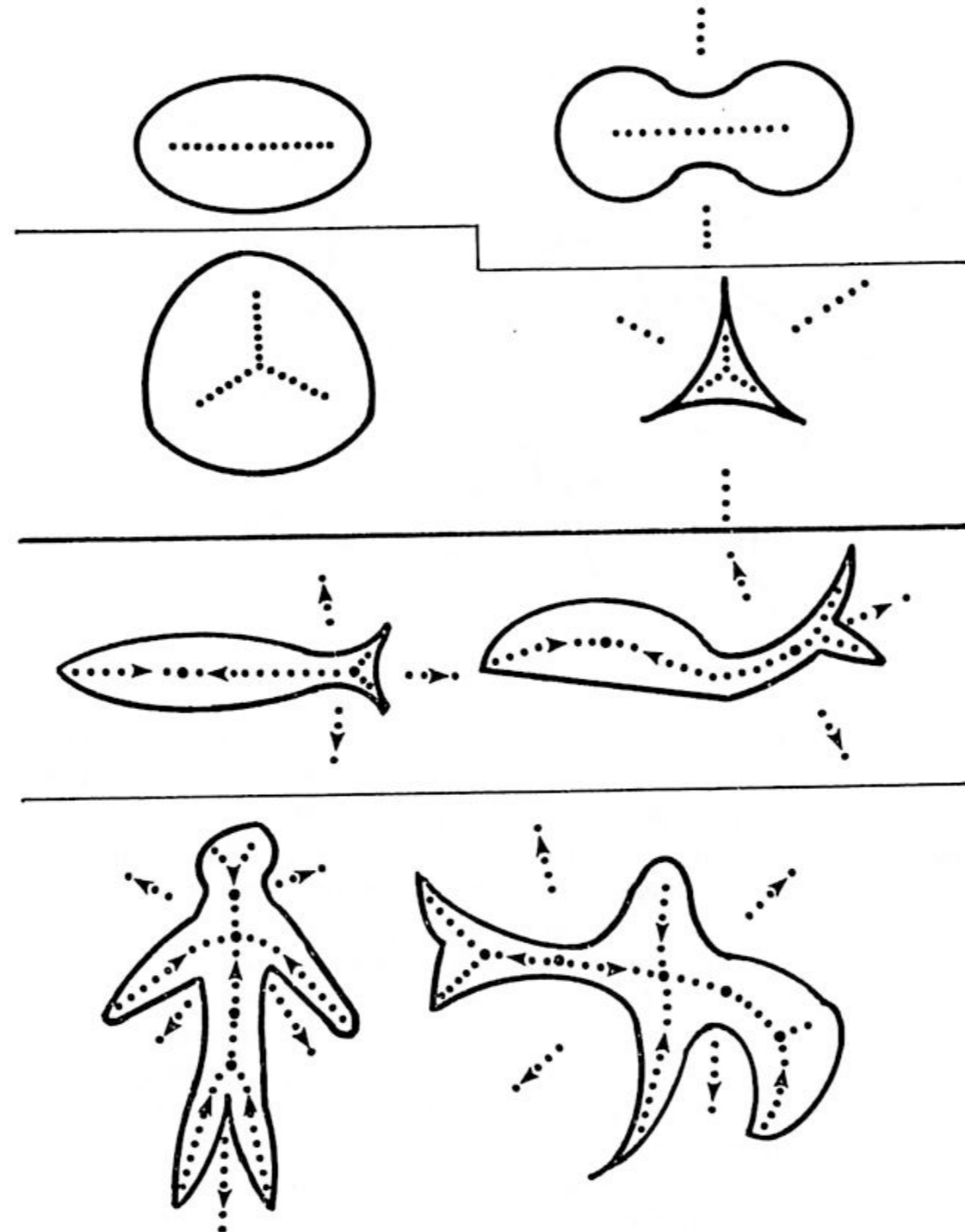


FIG. 29. Equivalent objects in some simple A-morphologies. In the upper half, the object sym-axes have the same topology. In the lower half, the object and ground have the same directed graph.

# Blum's A-Morphologies: 3D

BIOLOGICAL SHAPE

271

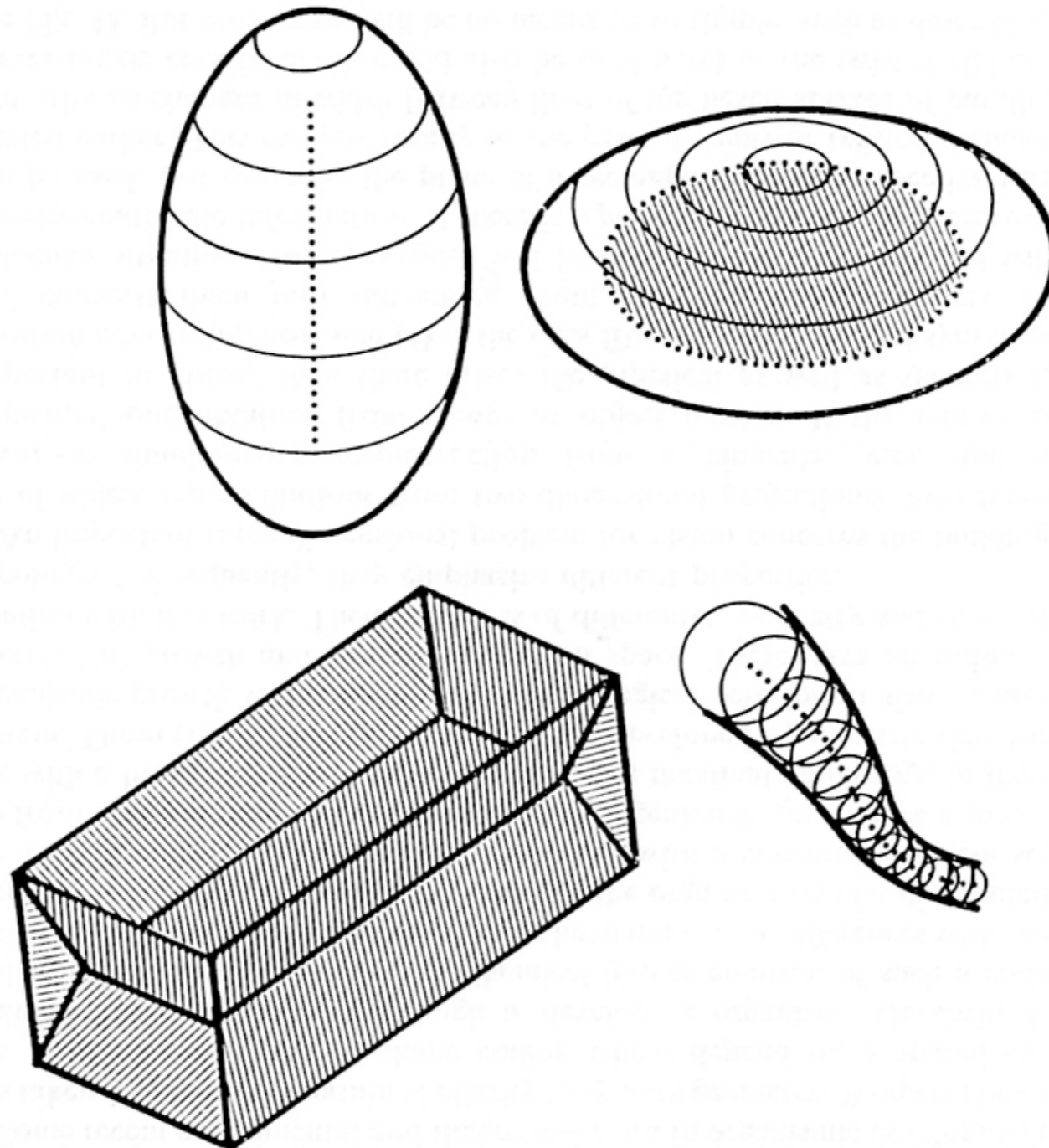
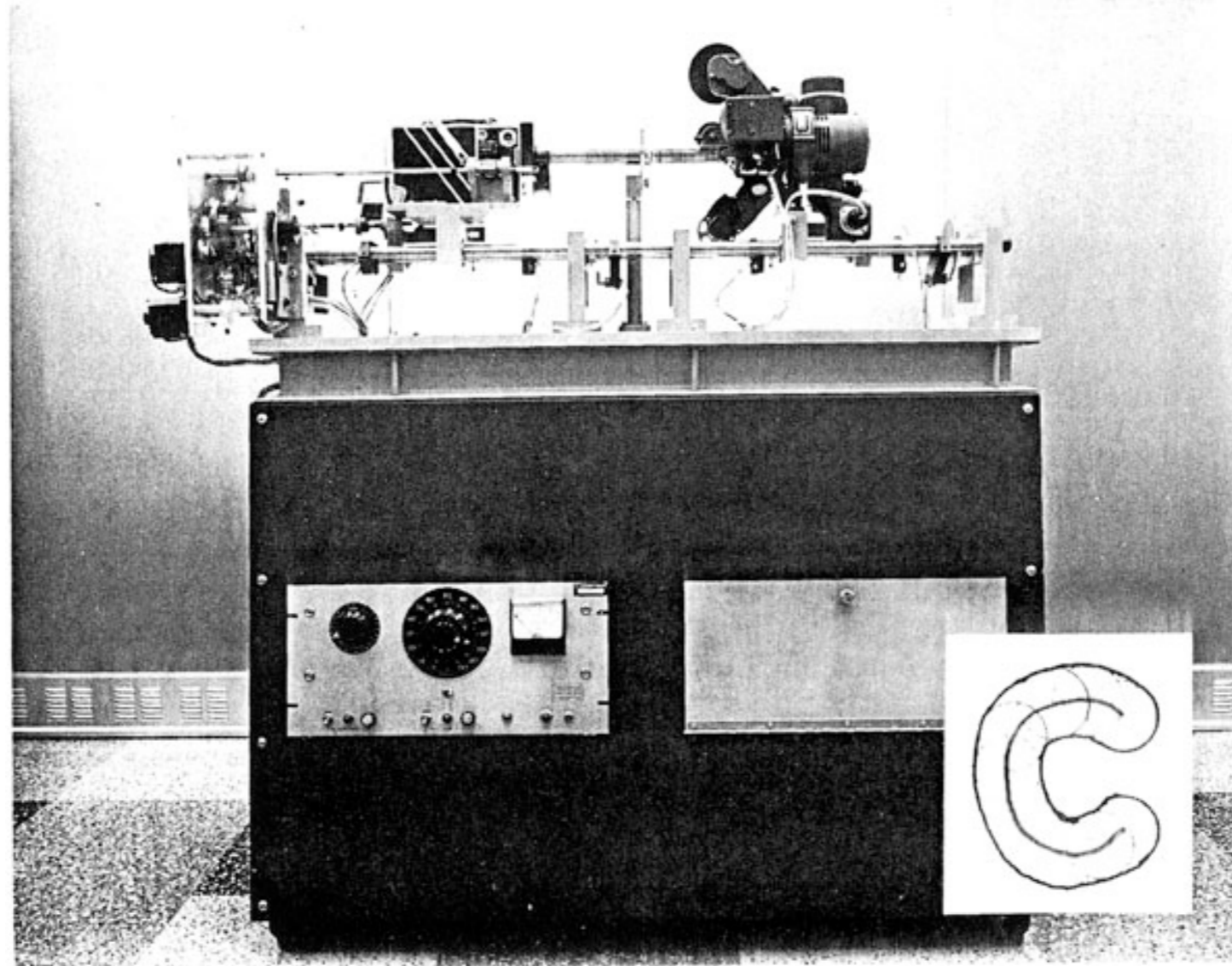


FIG. 42. Sym-axes of some three-dimensional objects. The ellipsoids at the top show that the sym-ax can now be both arcs and surfaces. The bottom shows the sym-ax for a rectangular solid and for a general spherical envelope.



# Blum's Grassfire Machine



"Figure 19 shows my first physical embodiment of the process. It uses a movie projector and camera with high contrast film. These are symmetrically driven apart from the lens in such a way as to keep a one to one magnification, but to increase the circle of confusion (defocussing). Corner detection is done by a separate process. I am presently building a closed loop electronic system to do both the wave generation and corner detection."

[A transformation for Extracting New Descriptors of Shape, 1967.]

Mathematics

# The Rowboat Analogy

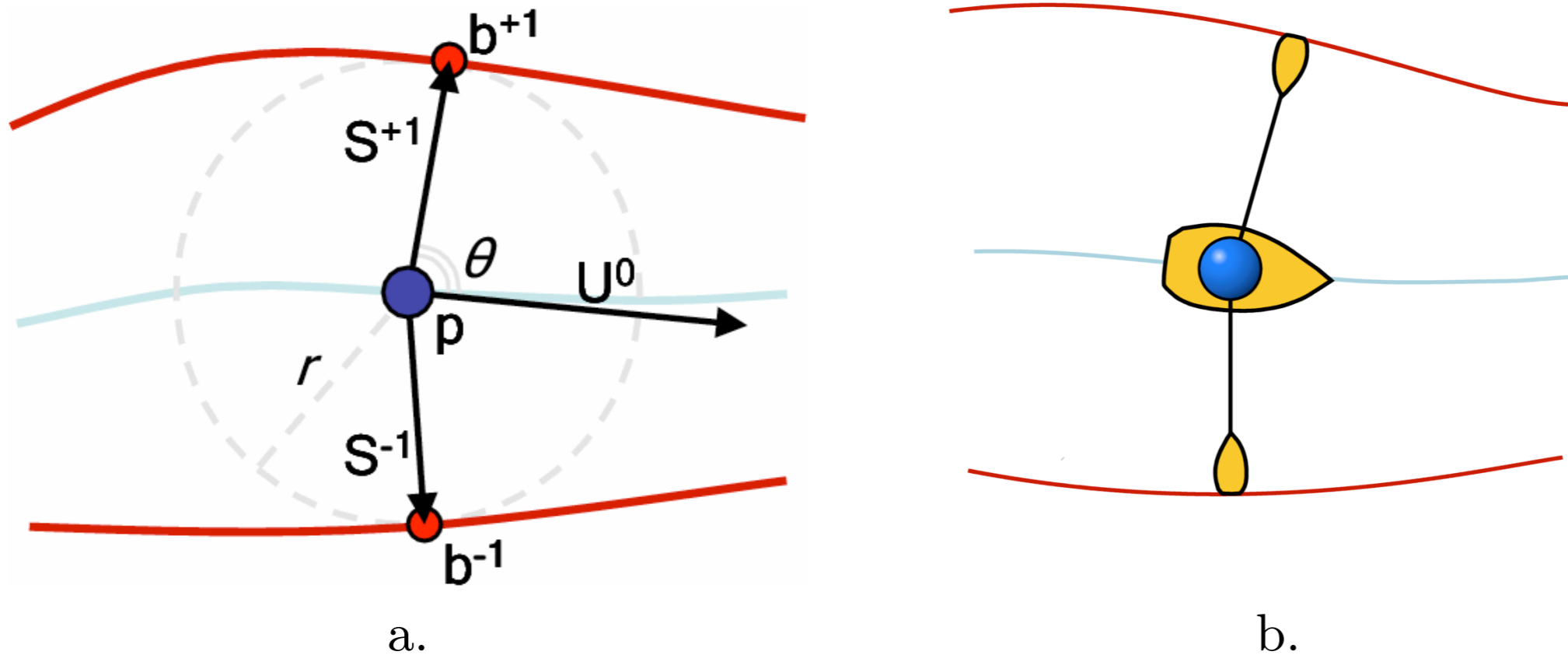
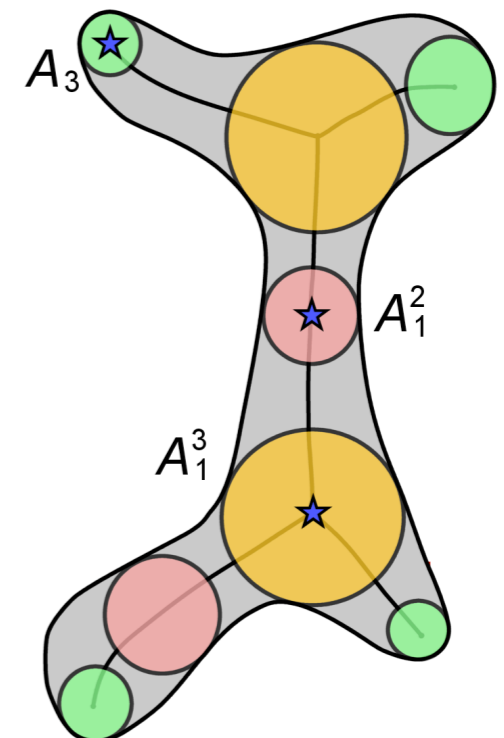
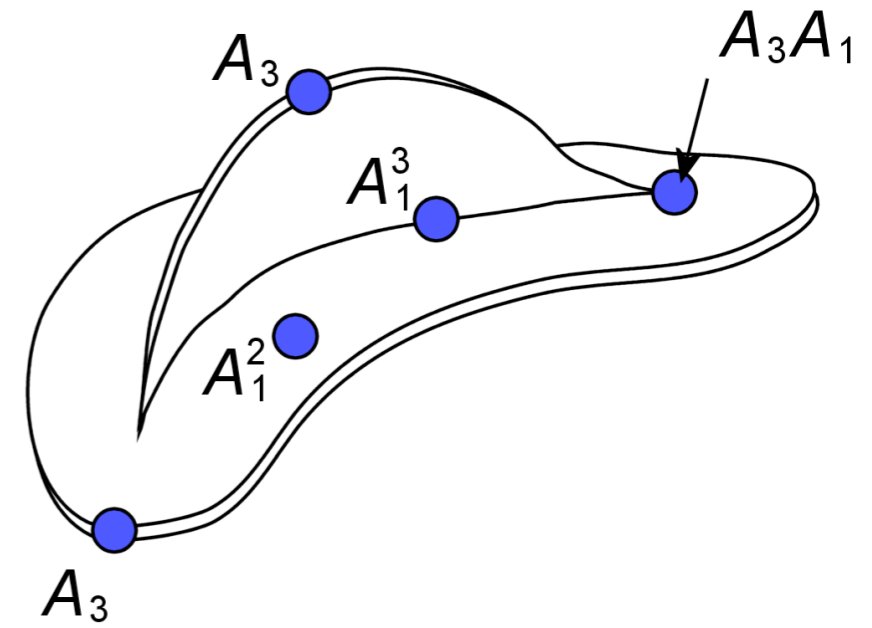


*Figure 1.7.* Local medial geometry. a. Local geometric properties of a medial point and its boundary pre-image. b. The rowboat analogy for medial points.

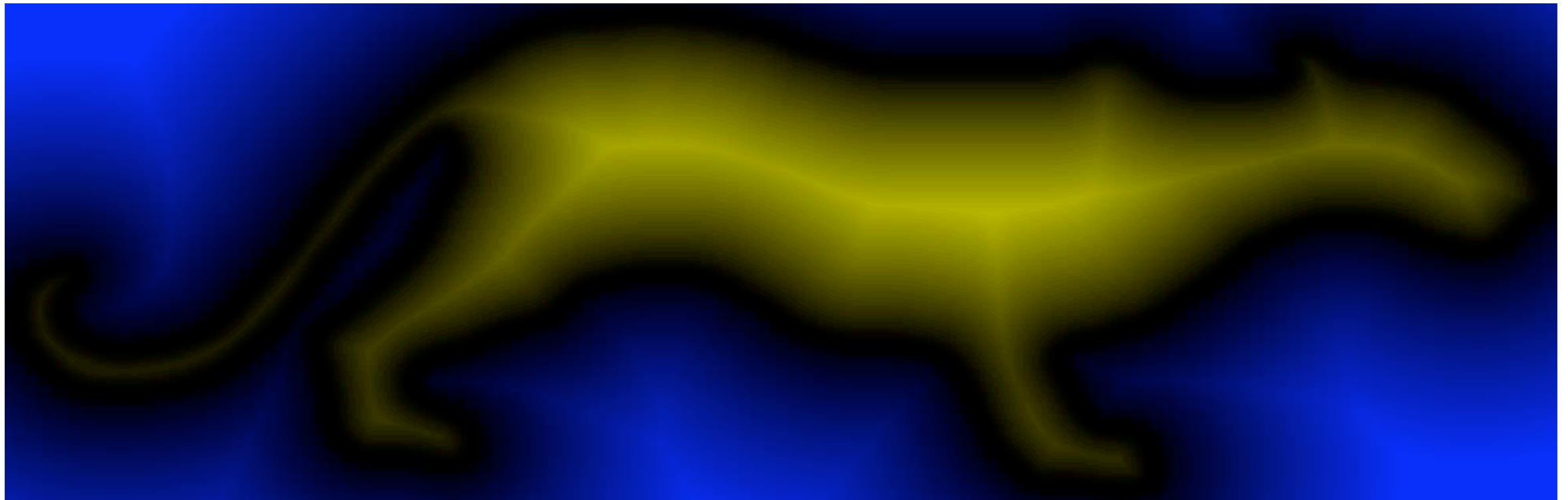
# Contact Classification

**Theorem 1 (Giblin and Kimia)** *The internal medial locus of a three-dimensional object  $\Omega$  generically consists of*

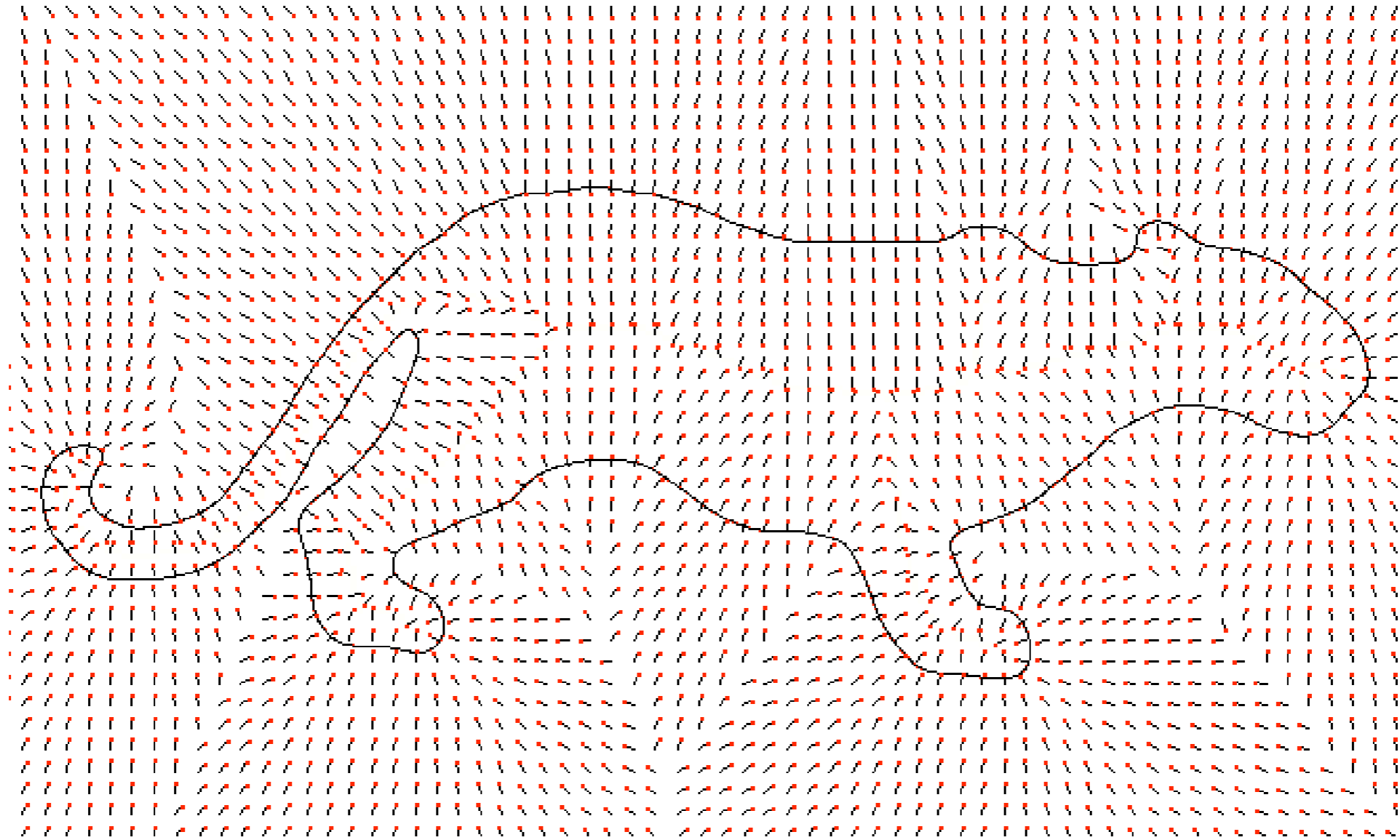
- 1 sheets (manifolds with boundary) of  $A_1^2$  medial points;
- 2 curves of  $A_1^3$  points, along which these sheets join, three at a time;
- 3 curves of  $A_3$  points, which bound the free (unconnected) edges of the sheets and for which the corresponding boundary points fall on a crest;
- 4 points of type  $A_1^4$ , which occur when four  $A_1^3$  curves meet;
- 5 points of type  $A_1A_3$  (i.e.,  $A_1$  contact and  $A_3$  contact at a distinct pair of points) which occur when an  $A_3$  curve meets an  $A_1^3$  curve.



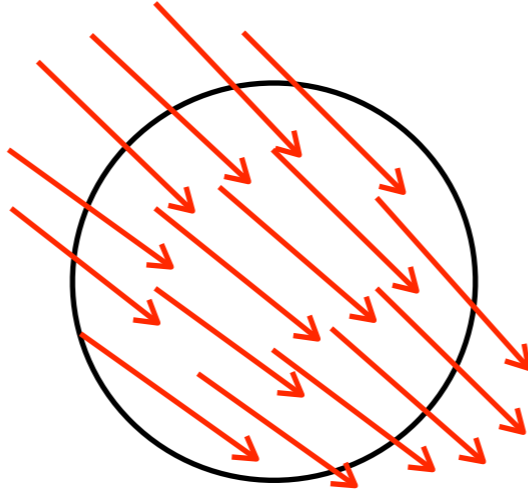
# Euclidean Distance Function



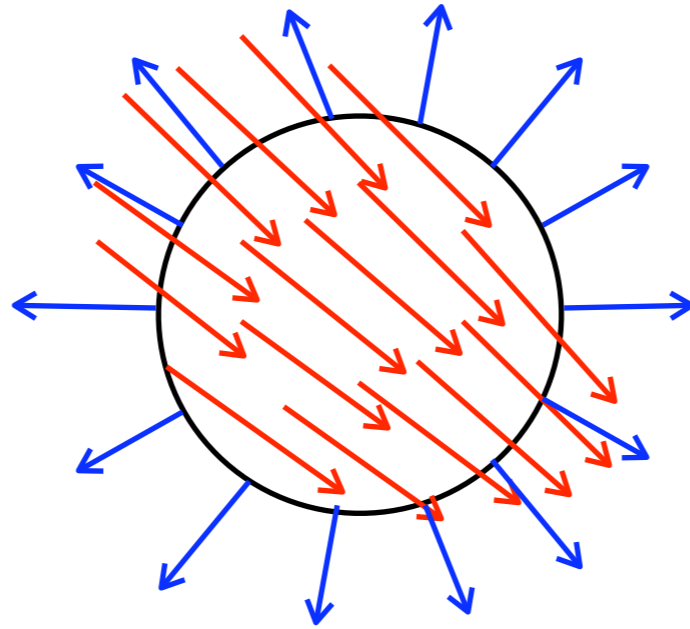
# Gradient Vector Field



# Outward Flux

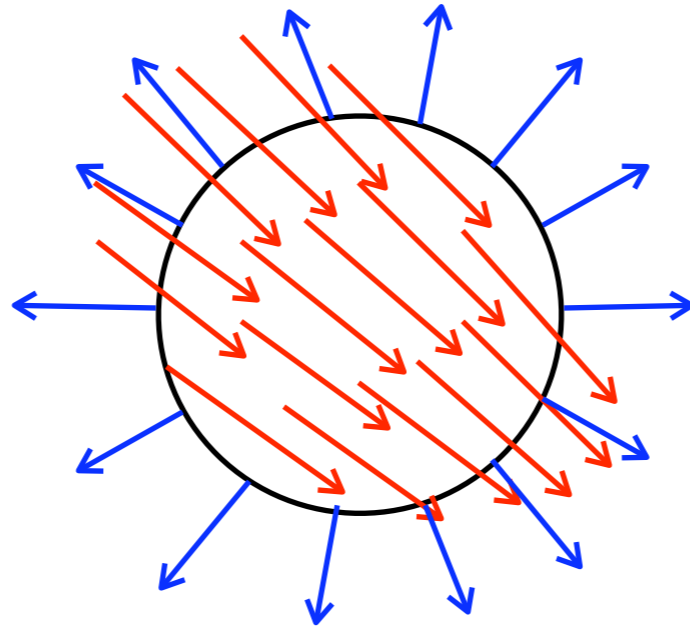


# Outward Flux





# Outward Flux

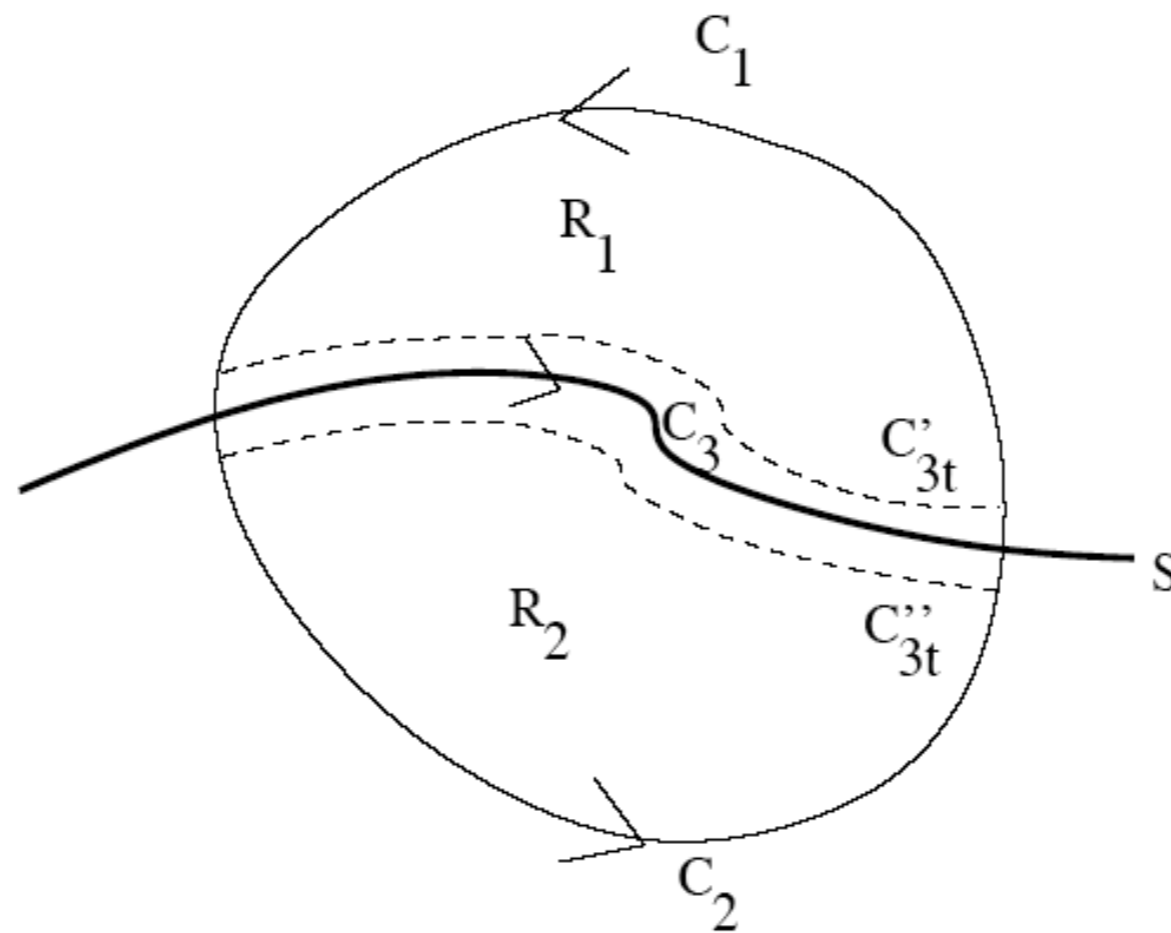


**Definition 1** *The outward flux of  $\dot{\mathbf{q}}$  through  $\partial R$  is given by*

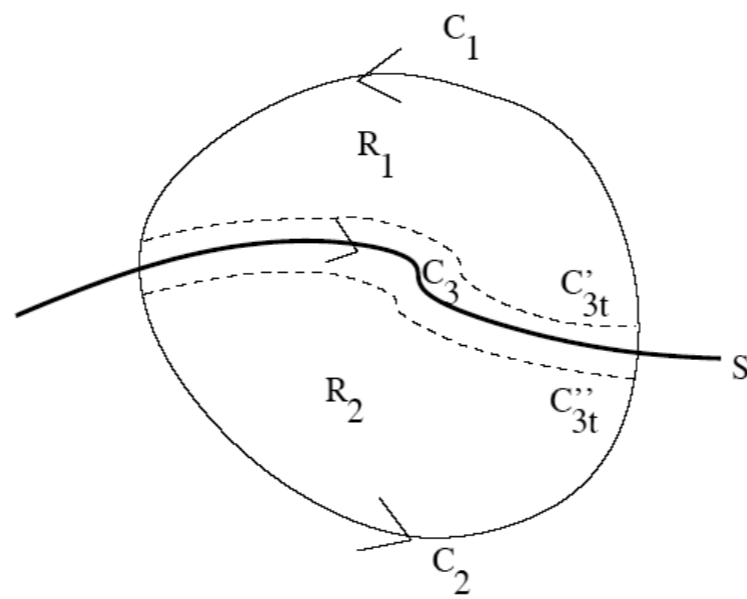
$$\int_{\partial R} \langle \dot{\mathbf{q}}, \mathcal{N} \rangle ds$$

**Definition 2** *The average outward flux of  $\dot{\mathbf{q}}$  through  $\partial R$  is given by*

$$\frac{\int_{\partial R} \langle \dot{\mathbf{q}}, \mathcal{N} \rangle ds}{\int_{\partial R} ds}$$



Let  $S$  be a branch of the skeleton and let  $R = R_1 \cup R_2$  be a path connected region which intersects it. Let  $\partial R = C_1 \cup C_2$  and  $C_3 = S \cap R$ . Let  $C'_{3t}, C''_{3t}$  be parallel curves to  $C_3$  which approach  $C_3$  as  $t \rightarrow 0$ . Let  $R_{1t}$  and  $R_{2t}$  be the regions obtained from  $R_1$  and  $R_2$  by removing the region between the curves  $C'_{3t}$  and  $C''_{3t}$ . Finally, let  $\dot{q}_+$  denote  $\dot{q}$  above  $S$  and  $\dot{q}_-$  denote  $\dot{q}$  below  $S$ .



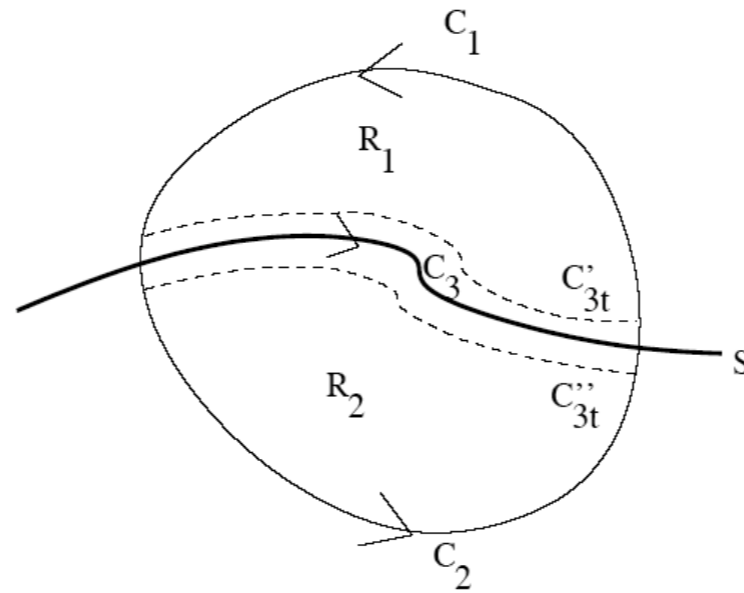
The outward flux of  $\dot{\mathbf{q}}$  through  $\partial R$  is given by

$$\int_{\partial R} \langle \dot{\mathbf{q}}, \mathcal{N} \rangle ds = \int_{C_1} \langle \dot{\mathbf{q}}, \mathcal{N} \rangle ds + \int_{C_2} \langle \dot{\mathbf{q}}, \mathcal{N} \rangle ds.$$

Applying the divergence theorem to  $R_{1t}$  and  $R_{2t}$

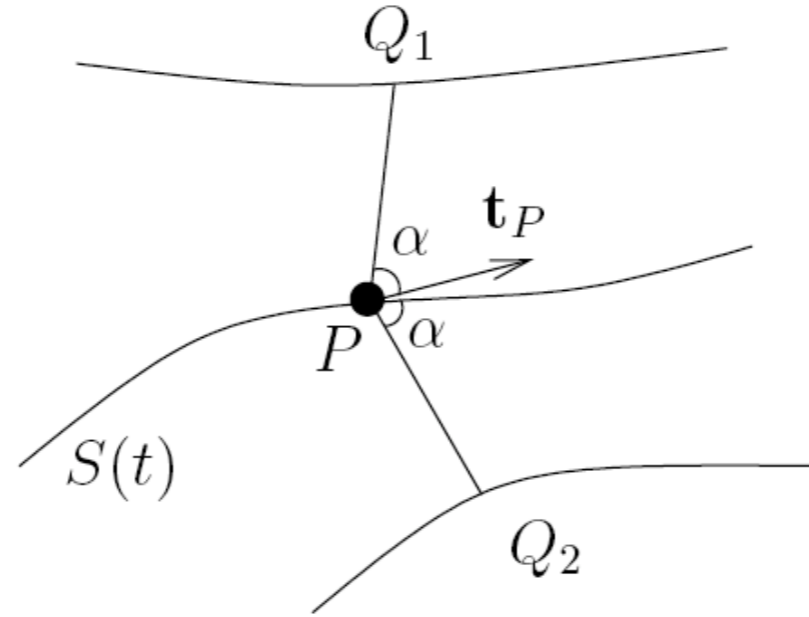
$$\int_{R_{1t}} \text{div}(\dot{\mathbf{q}}) dv = \int_{C_{1t}} \langle \dot{\mathbf{q}}, \mathcal{N} \rangle ds + \int_{C'_{3t}} \langle \dot{\mathbf{q}}, \mathcal{N} \rangle ds,$$

$$\int_{R_{2t}} \text{div}(\dot{\mathbf{q}}) dv = \int_{C_{2t}} \langle \dot{\mathbf{q}}, \mathcal{N} \rangle ds + \int_{-C''_{3t}} \langle \dot{\mathbf{q}}, \mathcal{N} \rangle ds.$$



Adding the above two equations we have

$$\begin{aligned}
 & \int_{R_{1t}} \operatorname{div}(\dot{\mathbf{q}}) \, dv + \int_{R_{2t}} \operatorname{div}(\dot{\mathbf{q}}) \, dv = \\
 & \int_{C_{1t}} \langle \dot{\mathbf{q}}, \mathcal{N} \rangle \, ds + \int_{C_{2t}} \langle \dot{\mathbf{q}}, \mathcal{N} \rangle \, ds + \\
 & \int_{C'_{3t}} \langle \dot{\mathbf{q}}, \mathcal{N} \rangle \, ds + \int_{-C''_{3t}} \langle \dot{\mathbf{q}}, \mathcal{N} \rangle \, ds.
 \end{aligned}$$



It is a standard property that the tangent to the skeleton bisects the angle between  $\dot{\mathbf{q}}_+$  and  $\dot{\mathbf{q}}_-$  at a skeletal point (see Figure 2). Thus, on  $C_3$  we have

$$\langle \dot{\mathbf{q}}_+, \mathcal{N}_+ \rangle = \langle \dot{\mathbf{q}}_-, \mathcal{N}_- \rangle, \quad (2)$$

where  $\mathcal{N}_+, \mathcal{N}_-$  denote the normals to  $C_3$  from above and from below, respectively. Thus, one can take the limit as  $t \rightarrow 0$  of both sides of the above equation to obtain the following extension of the divergence theorem

# (extended) Divergence Theorem

**Theorem 1** *For a path connected region  $R$  which contains part of a skeletal curve  $S$ , the divergence of the vector field  $\dot{\mathbf{q}}$  is related to its flux through  $\partial R$  by the following equation*

$$\int_{R=R_1 \cup R_2} \operatorname{div}(\dot{\mathbf{q}}) \, dv = \int_{\partial R} \langle \dot{\mathbf{q}}, \mathcal{N} \rangle \, ds + 2 \int_{C_3} \langle \dot{\mathbf{q}}, \mathcal{N}_{C_3} \rangle \, ds.$$

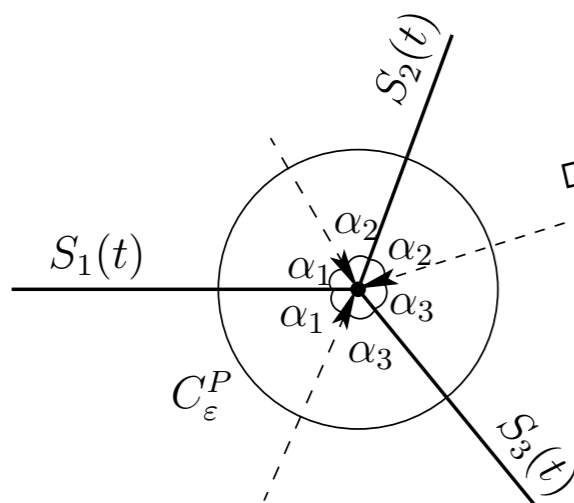
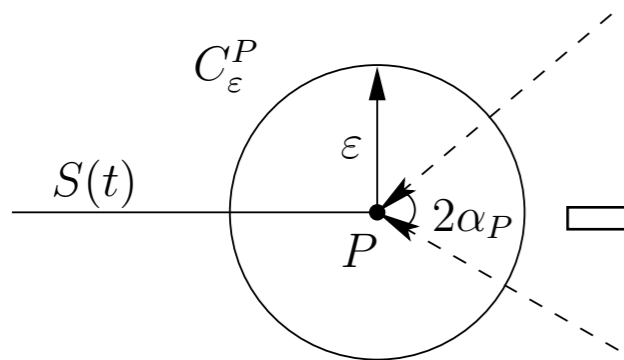
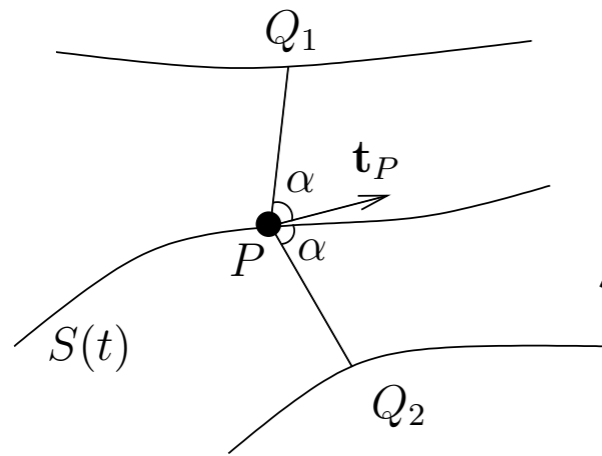
**Corollary.** *The OF for a region shrinking to a skeleton point satisfies:*

$$\lim_{R \rightarrow P} \operatorname{OF}_R \rightarrow 2 (\langle \nabla D(P), \mathcal{N} \rangle) \operatorname{length}(C_3)$$

# Circular Neighborhoods

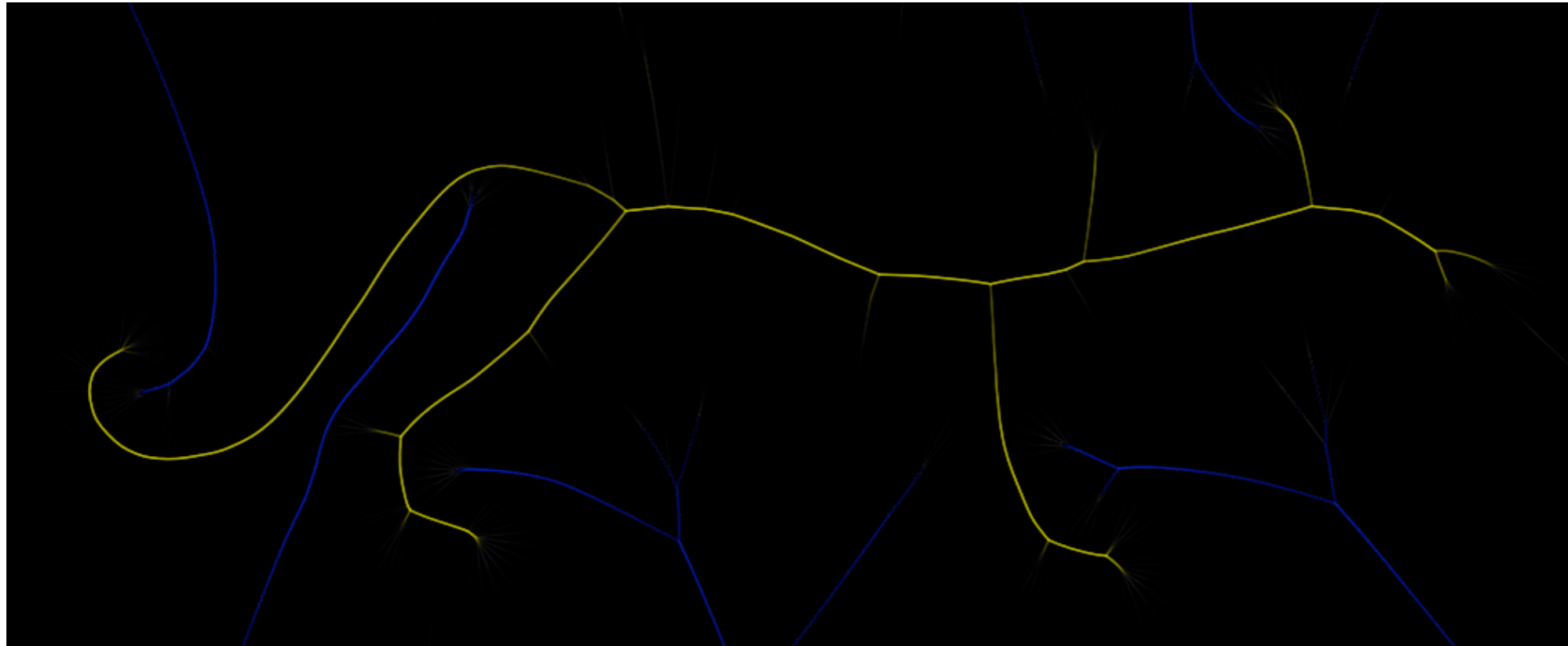
(Dimitrov, Damon, Siddiqi, CVPR'03)

The AOF for shrinking circular regions:



$R \rightarrow P$	$\text{AOF}_R \rightarrow x$
Regular Points	$-\frac{2}{\pi} \sin \alpha$
End-Points	$-\frac{1}{\pi} (\sin \alpha + \alpha)$
Junction Points	$-\frac{1}{\pi} \sum_{i=1}^n \sin \alpha_i$
Non-Skeletal Points	0

# Average Outward Flux





# Damon: Skeletal Structures

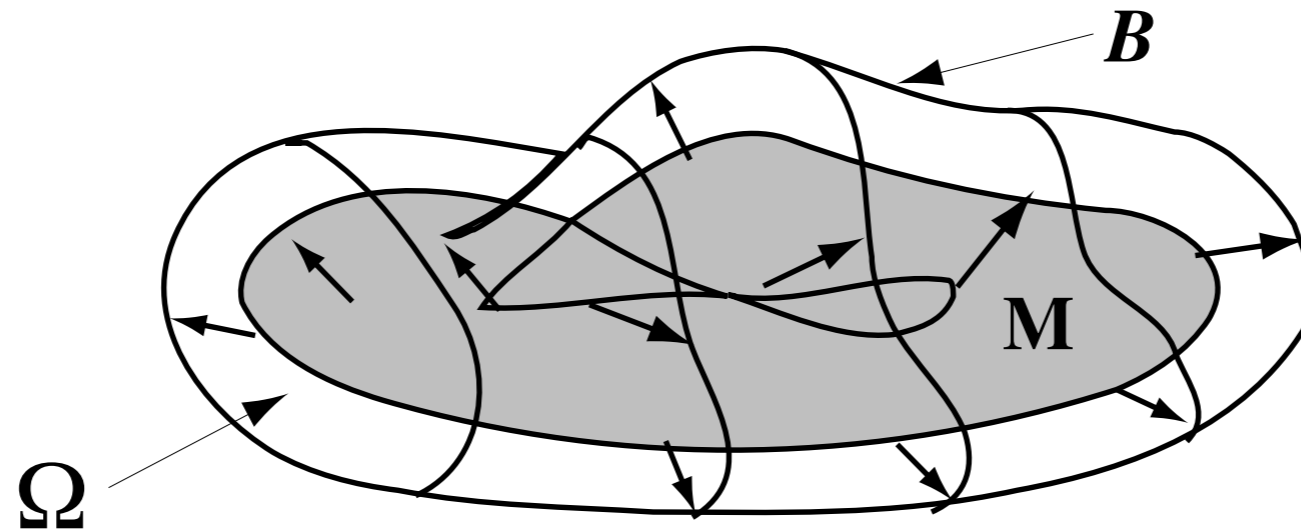


FIGURE 2. A Skeletal Structure  $(M, U)$  defining a region  $\Omega$  with smooth boundary  $B$

*radial shape operator*

$$S_{rad}(v) = -\text{proj}_U\left(\frac{\partial U_1}{\partial v}\right)$$

*radial curvature*

$$K_{rad} = \det(S_{rad})$$

# Damon: Radial Flow

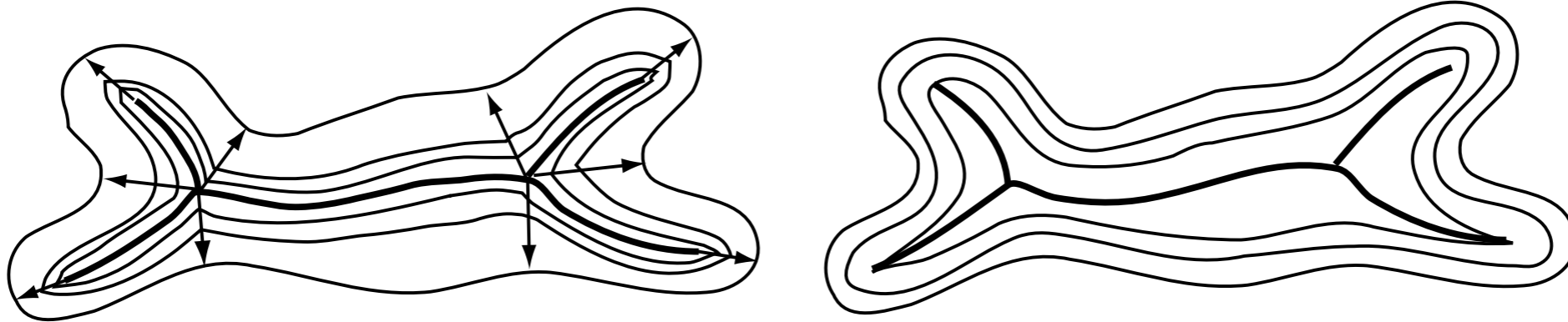


FIGURE 3. a) Radial Flow and b) Grassfire Flow

- radial curvature condition + edge condition + compatibility condition ensure smoothness of boundary
- complete characterization of local and relative differential geometry of boundary in terms of radial shape operator on skeletal structure

# (Rigorous) Divergence Theorem

**Theorem 9** (Modified Divergence Theorem). *Let  $\Omega$  be a region with smooth boundary  $\mathcal{B}$  defined by the skeletal structure. Also, let  $\Gamma$  be a region in  $\Omega$  with regular piecewise smooth boundary. Suppose  $F$  is a smooth vector field with discontinuities across  $M$ , then*

$$(7.1) \quad \int_{\Gamma} \operatorname{div} F \, dV = \int_{\partial\Gamma} F \cdot \mathbf{n}_{\Gamma} \, dS - \int_{\tilde{\Gamma}} c_F \, dM$$

where  $\tilde{\Gamma} = \tilde{M} \cap \pi^{-1}(M \cap \Gamma)$ .

$\operatorname{proj}_{TM}(F) = c_F \cdot U_1$ , where  $\operatorname{proj}_{TM}$  denotes projection onto  $U$  along  $TM$

# Boundary Integrals as Medial Integrals

**Theorem 1.** *Suppose  $(M, U)$  is a skeletal structure defining a region with smooth boundary  $\mathcal{B}$  and satisfying the partial Blum condition. Let  $g : \mathcal{B} \rightarrow \mathbb{R}$  be Borel measurable and integrable with respect to the Riemannian volume measure. Then,*

$$(3.1) \quad \int_{\mathcal{B}} g \, dV = \int_{\tilde{M}} \tilde{g} \cdot \det(I - rS_{rad}) \, dM$$

where  $\tilde{g} = g \circ \psi_1$ .

# Algorithms

# Algorithm

---

**Algorithm 2:** Topology Preserving Thinning.

---

**Data** : Object, Average Outward Flux Map.

**Result** : (2D or 3D) Skeleton.

```
for (each point  $\mathbf{x}$  on the boundary of the object) do  
    if ( $\mathbf{x}$  is simple) then  
        | insert( $\mathbf{x}$ , maxHeap) with AOF( $\mathbf{x}$ ) as the sorting key for insertion;  
while (maxHeap.size > 0) do  
    |  $\mathbf{x}$  = HeapExtractMax(maxHeap);  
    | if ( $\mathbf{x}$  is simple) then  
    | | if ( $\mathbf{x}$  is an end point) and (AOF( $\mathbf{x}$ ) < Thresh) then  
    | | | mark  $\mathbf{x}$  as a medial surface (end) point;  
    | | else  
    | | | Remove  $\mathbf{x}$ ;  
    | | | for (all neighbors  $\mathbf{y}$  of  $\mathbf{x}$ ) do  
    | | | | if ( $\mathbf{y}$  is simple) then  
    | | | | | insert( $\mathbf{y}$ , maxHeap) with AOF( $\mathbf{y}$ ) as the sorting key for in-  
    | | | | | sertion;
```

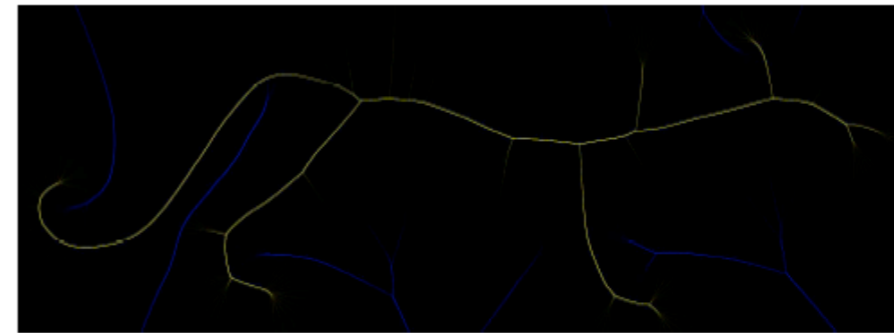
---

# Validation

To verify the theoretical results, boundary points corresponding to regular skeletal points are reconstructed according to:  $Q_{1,2} = P + rR(\pm\alpha)\mathbf{t}_P$



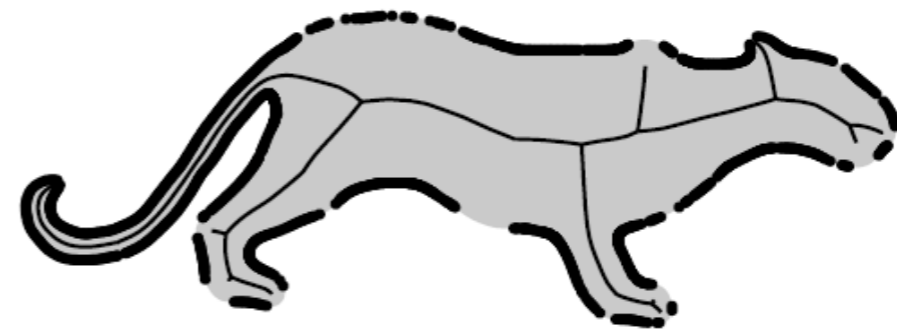
**STEP 1.** Start with a binary shape.



**STEP 2.** Compute AOF of shape using circular regions.



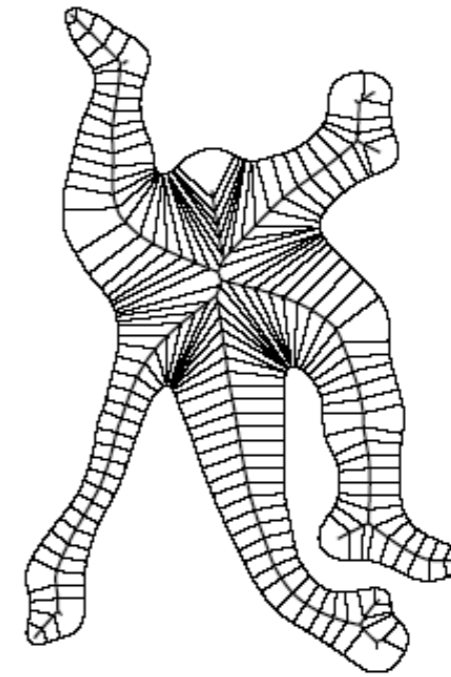
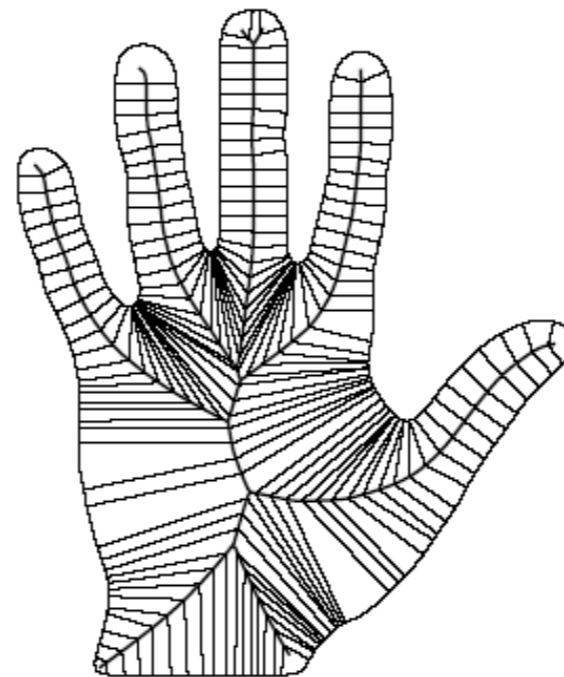
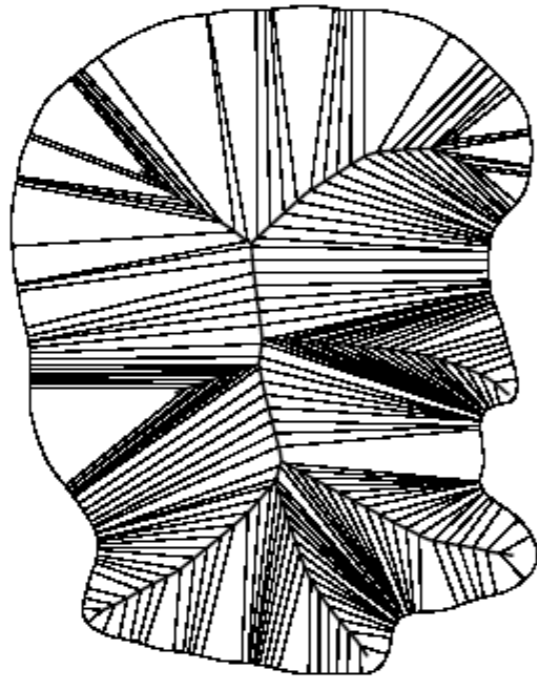
**STEP 3.** Compute skeleton with algorithm presented in [3].



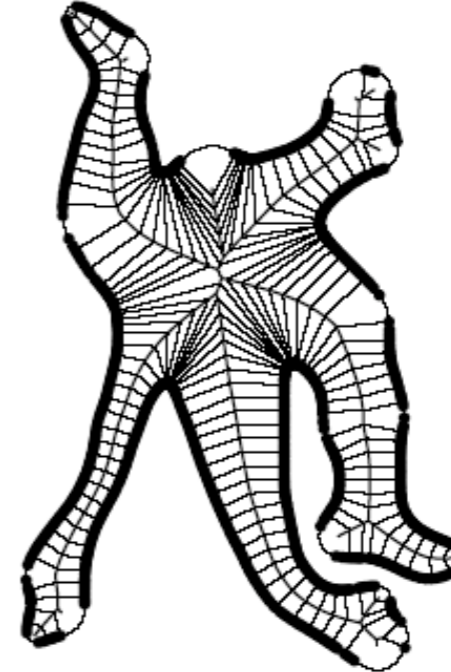
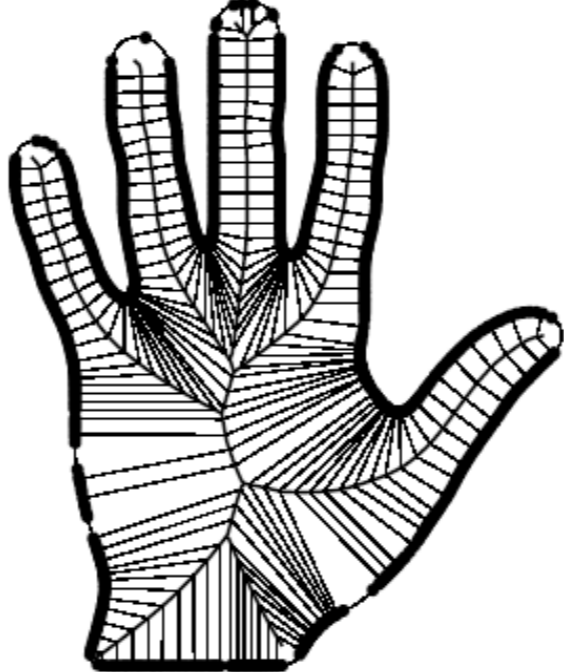
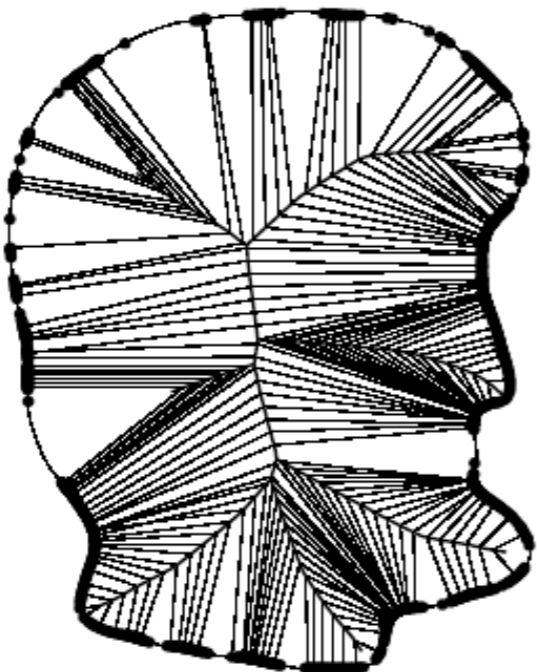
**STEP 4.** Using our results for shrinking circular regions, reconstruct boundary points from regular skeletal points.

# Validation

Ground  
Truth



Reconstruction



The limiting average outward flux value determines the object angle, which in turn is used to recover the associated bi-tangent points, shown as filled circles.



# Brain Ventricles



Original

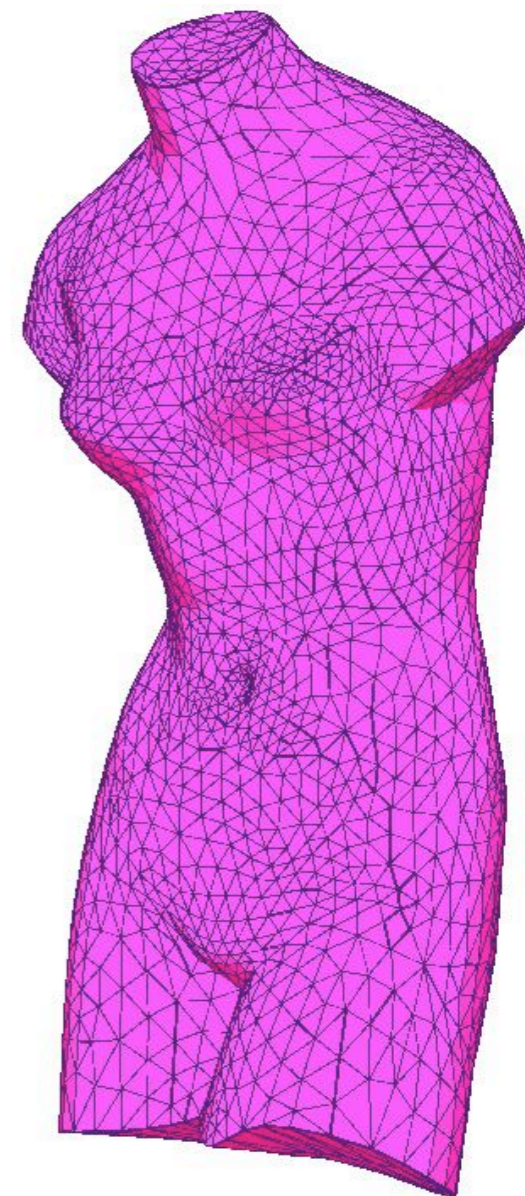
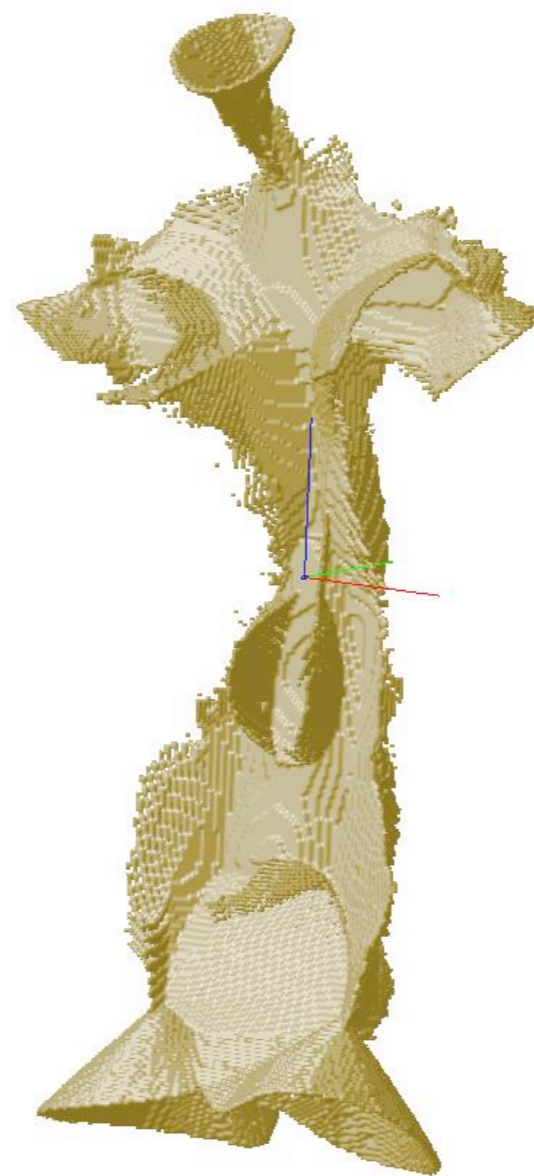
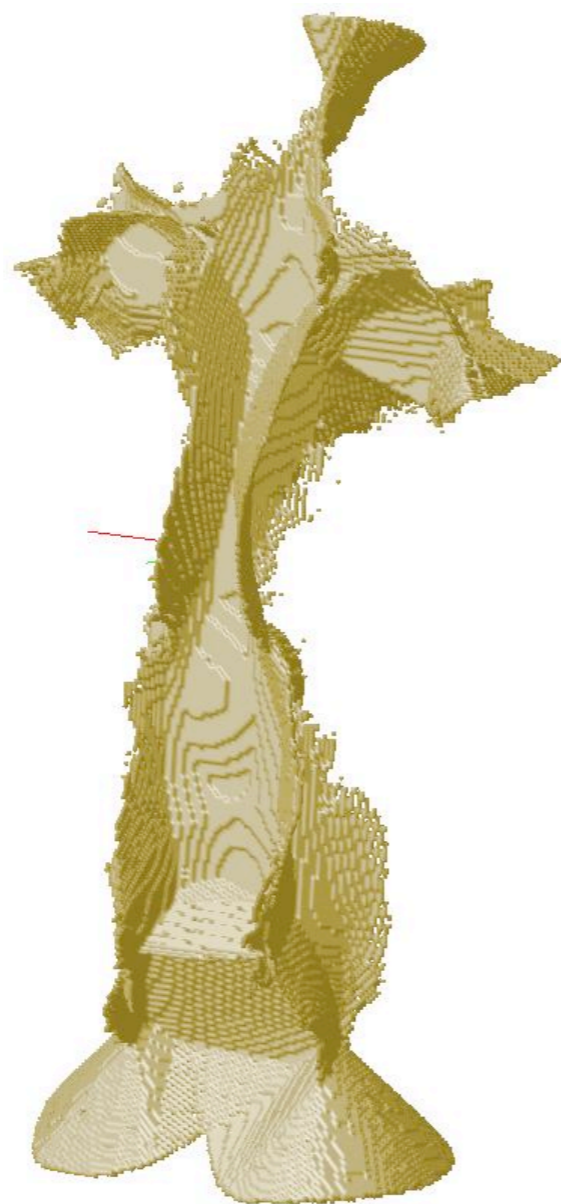


Medial Surface

# Venus de Milo

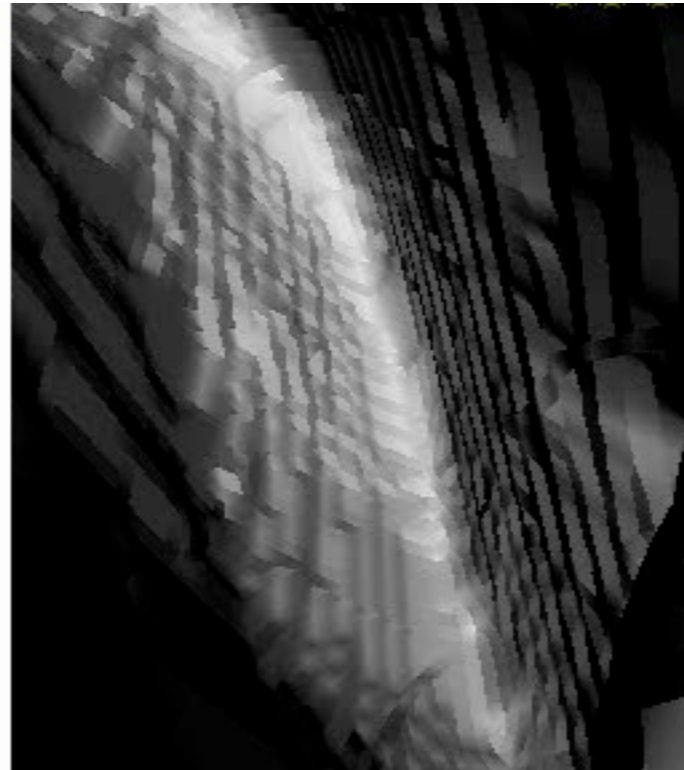
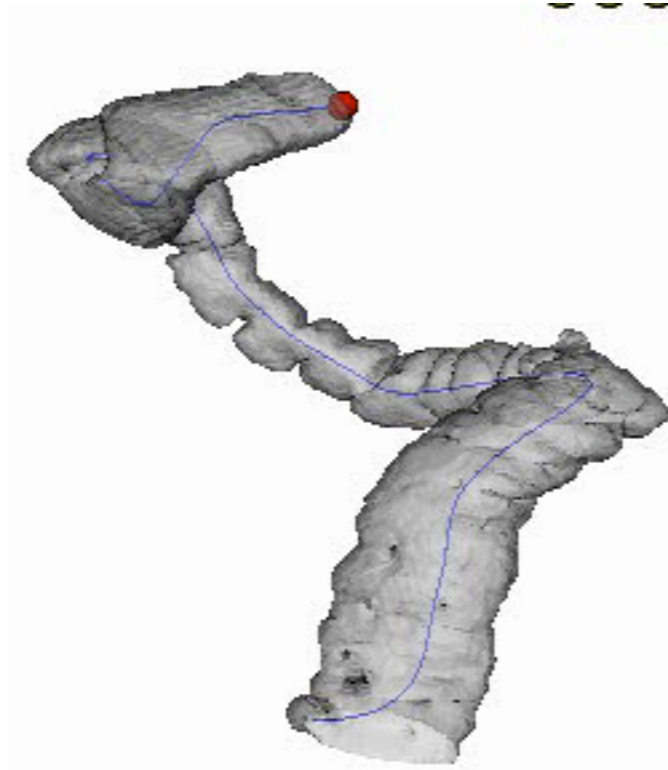


Circa 100 BC

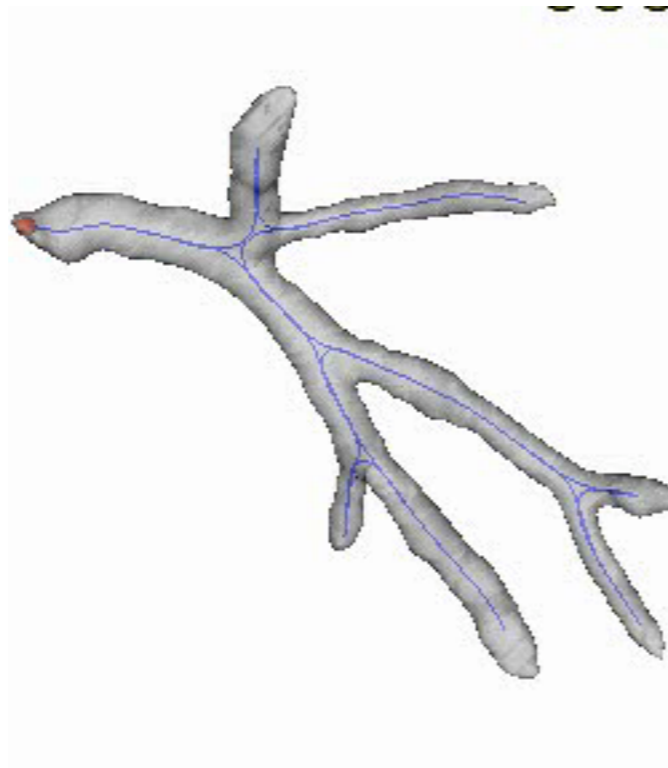


Applications

# Virtual Endoscopy

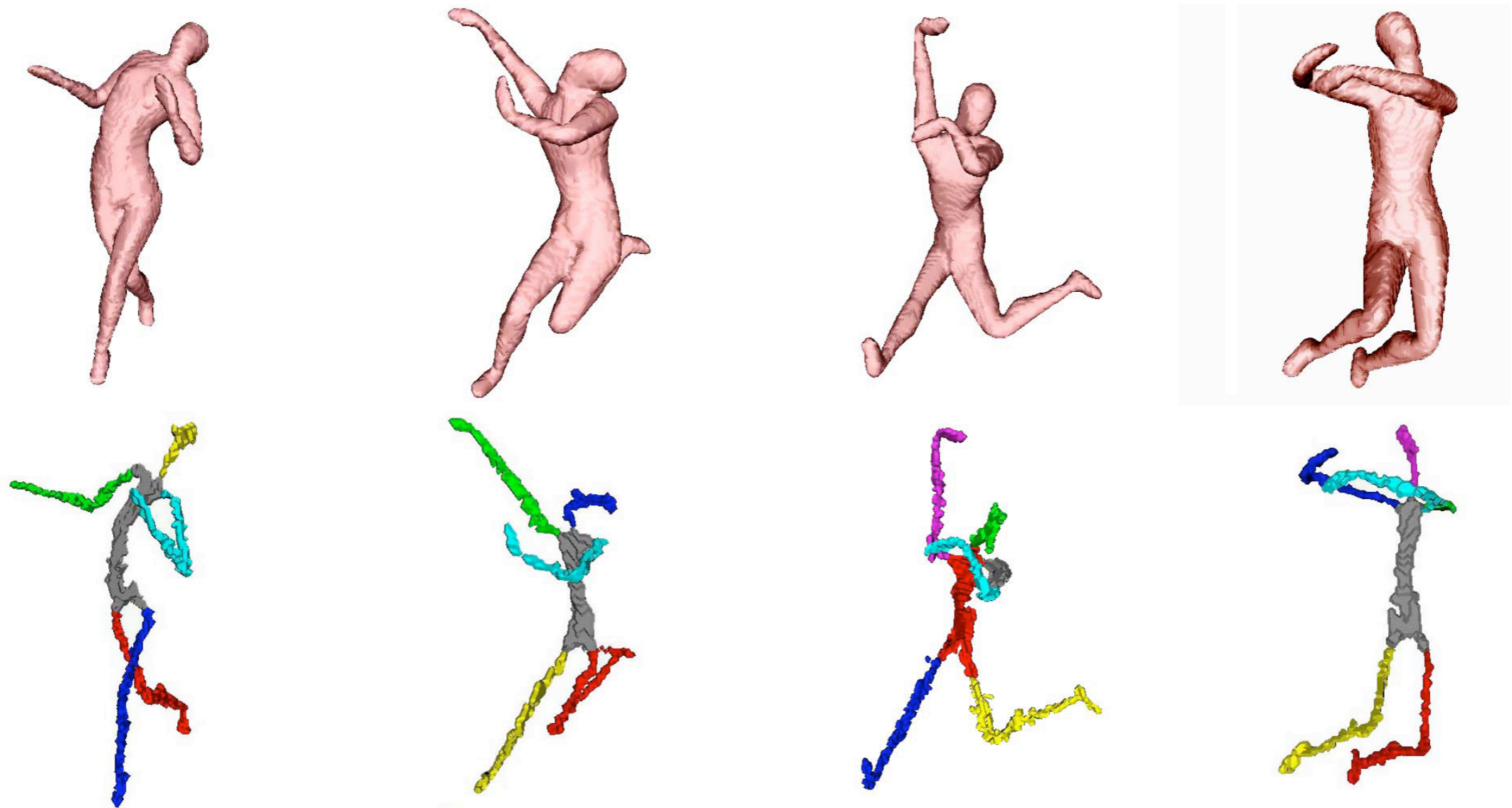


Colon



Arteries

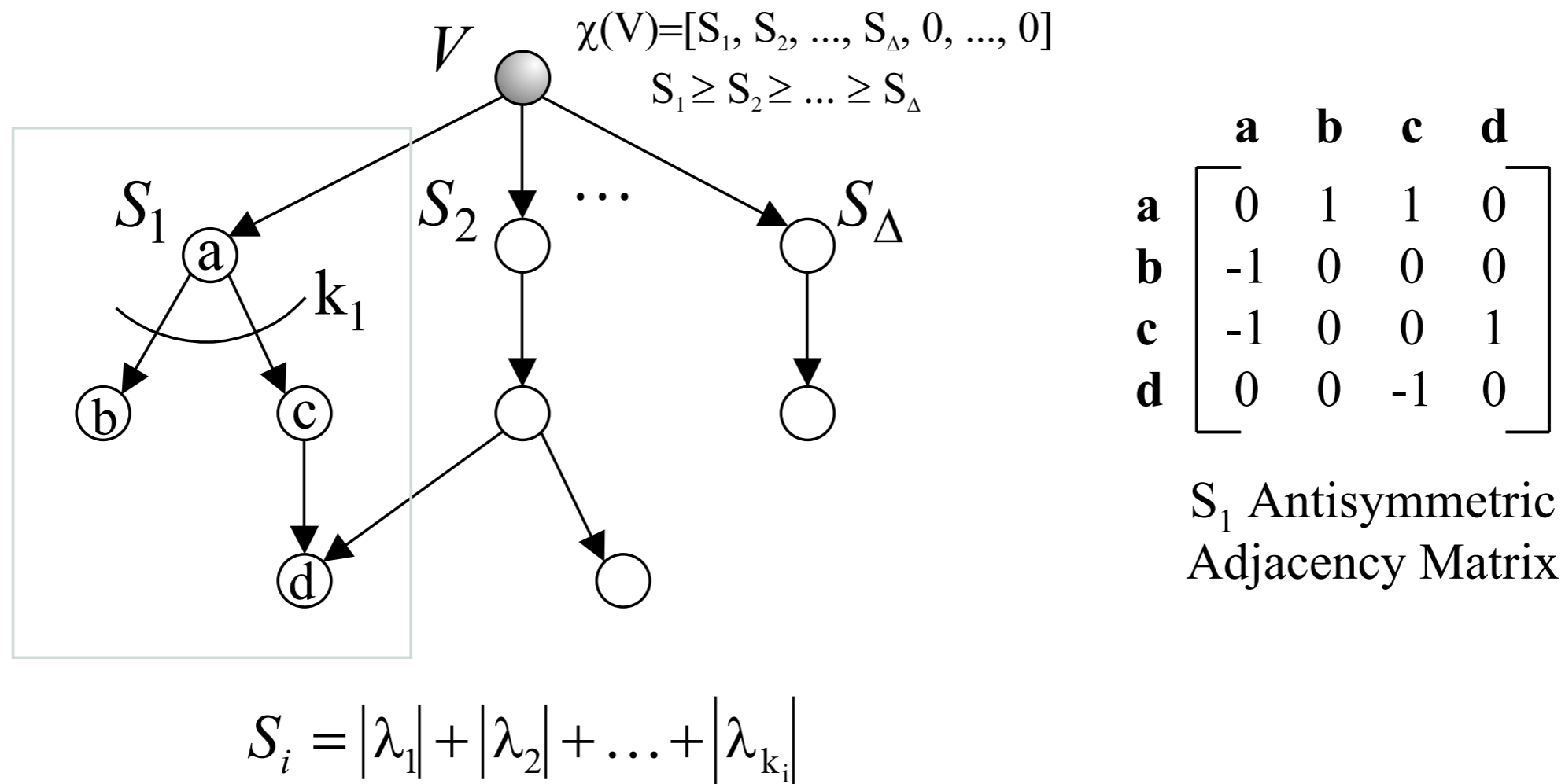
# 3D Medial Graph Matching



# Medial Graph Matching

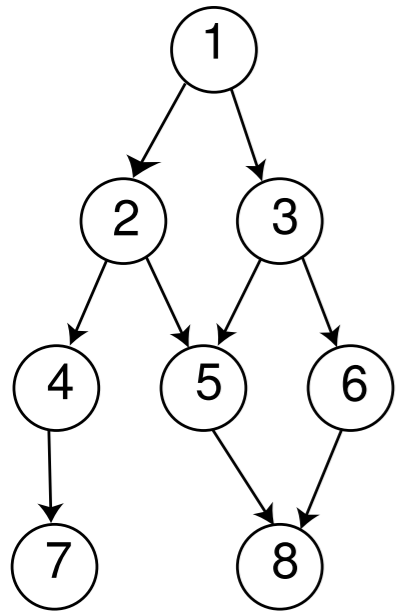
- Edit Distance Based Approaches  
(Sebastian, Kline, Kimia; Hancock, Torsello)
  - motivated by string edit distances
  - polynomial time algorithm for trees, (but need to define edit costs)
- Maximum Clique Approaches  
(Pelillo et al.)
  - subgraph isomorphism → maximum clique in an association graph
  - discrete combinatorial problem → continuous optimization
- Graph Spectra-Based Approaches  
(Shokoufandeh et al.)
  - eigenvalue analysis of adjacency matrix for DAGs
  - separation of “topology” and “geometry”
  - extension to handle indexing

# A Topological Signature Vector

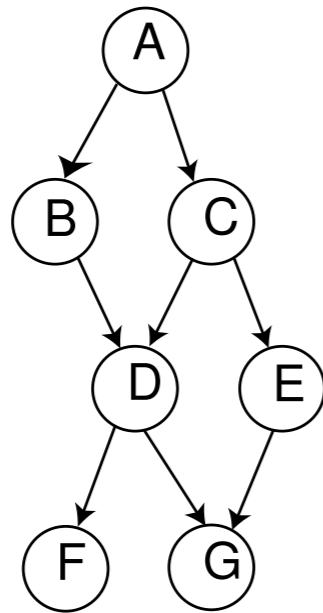


- At node "a" compute the sum of the magnitudes of the "k" largest eigenvalues of the adjacency matrix of the subgraph rooted at "a".
- Carry out this process recursively at all nodes.
- The sorted sums become the components of the "TSV" assigned to node V.

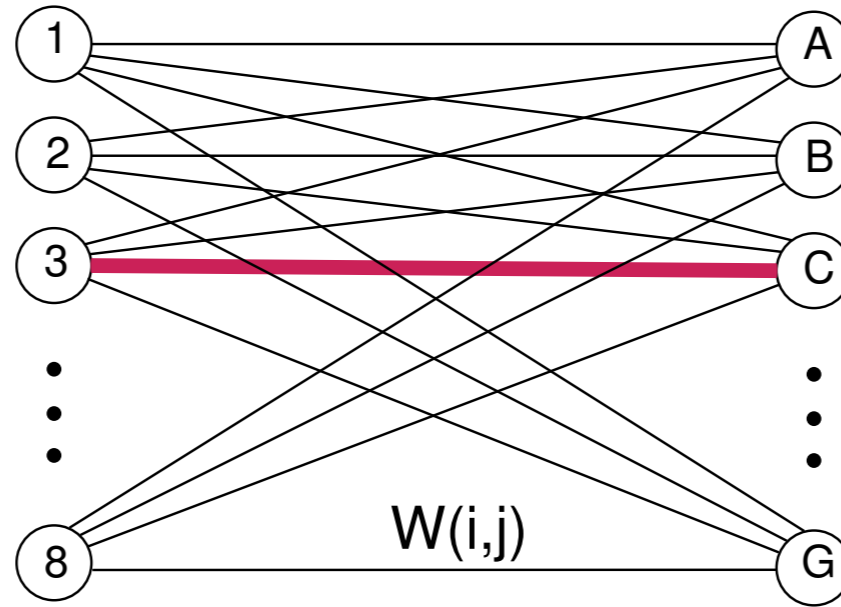
# Matching Algorithm



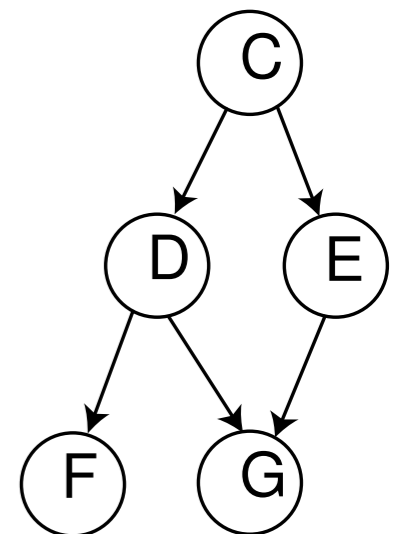
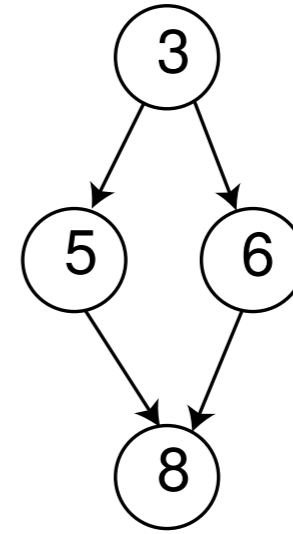
(a)



(b)



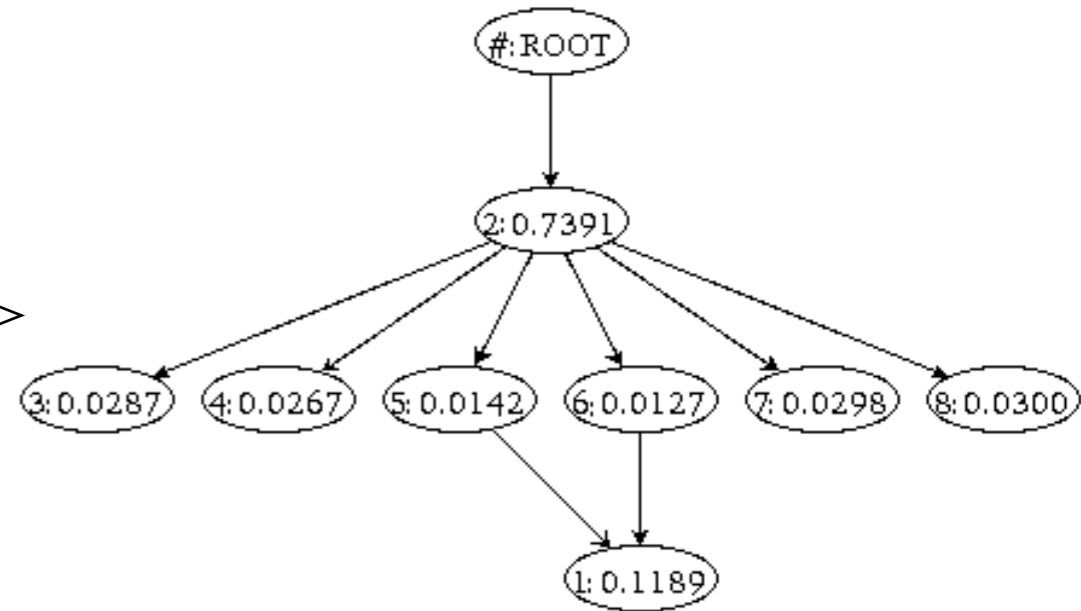
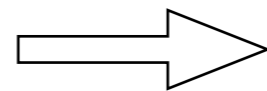
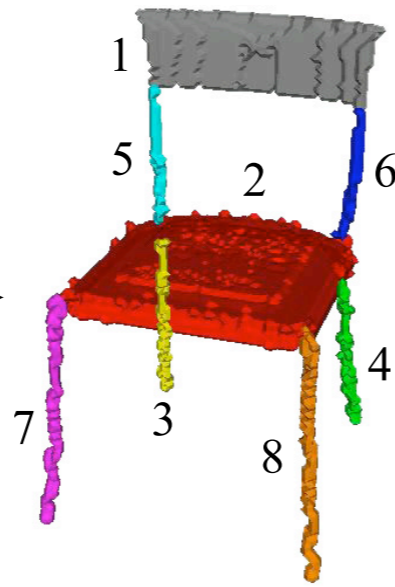
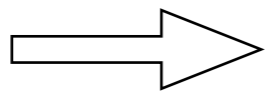
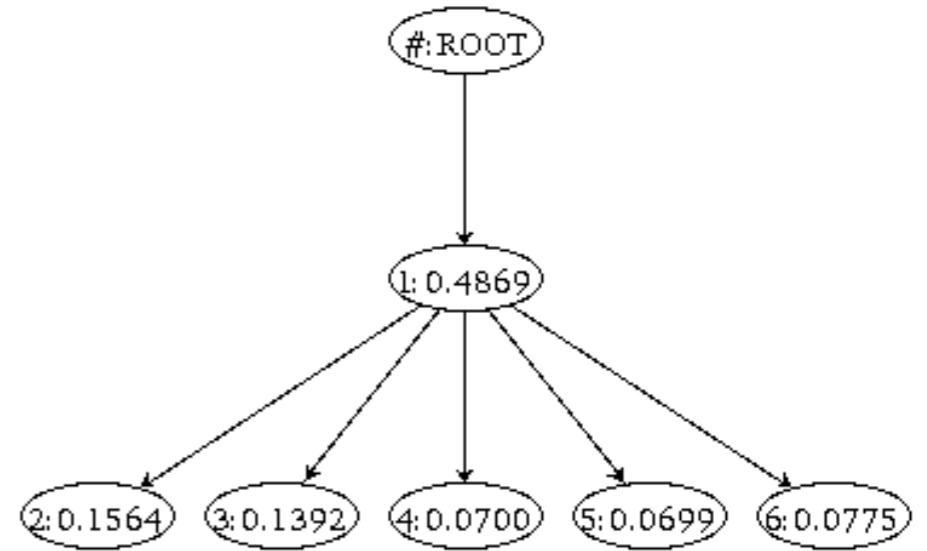
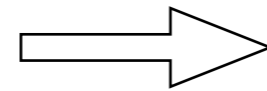
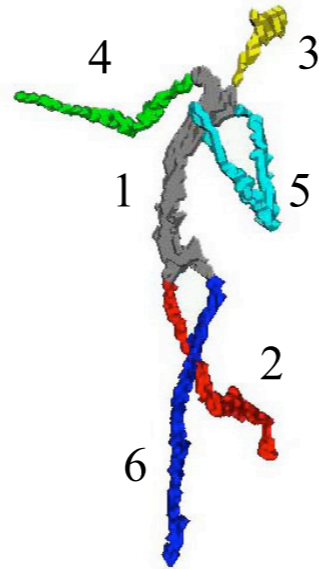
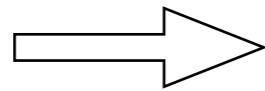
(c)



- (a) Two DAGs to be matched.
- (b) A bi-partite graph is formed, spanning their nodes but excluding their edges. The edge weights  $W(i,j)$  in the bi-partite graph encode node similarity as well as TSV similarity. The two most similar nodes are found, and are added to the solution set of correspondences.
- (c) This process is applied, recursively, to the subgraphs of the two most similar nodes. This ensures that the search for corresponding nodes is focused in corresponding subgraphs, in a top-down manner.



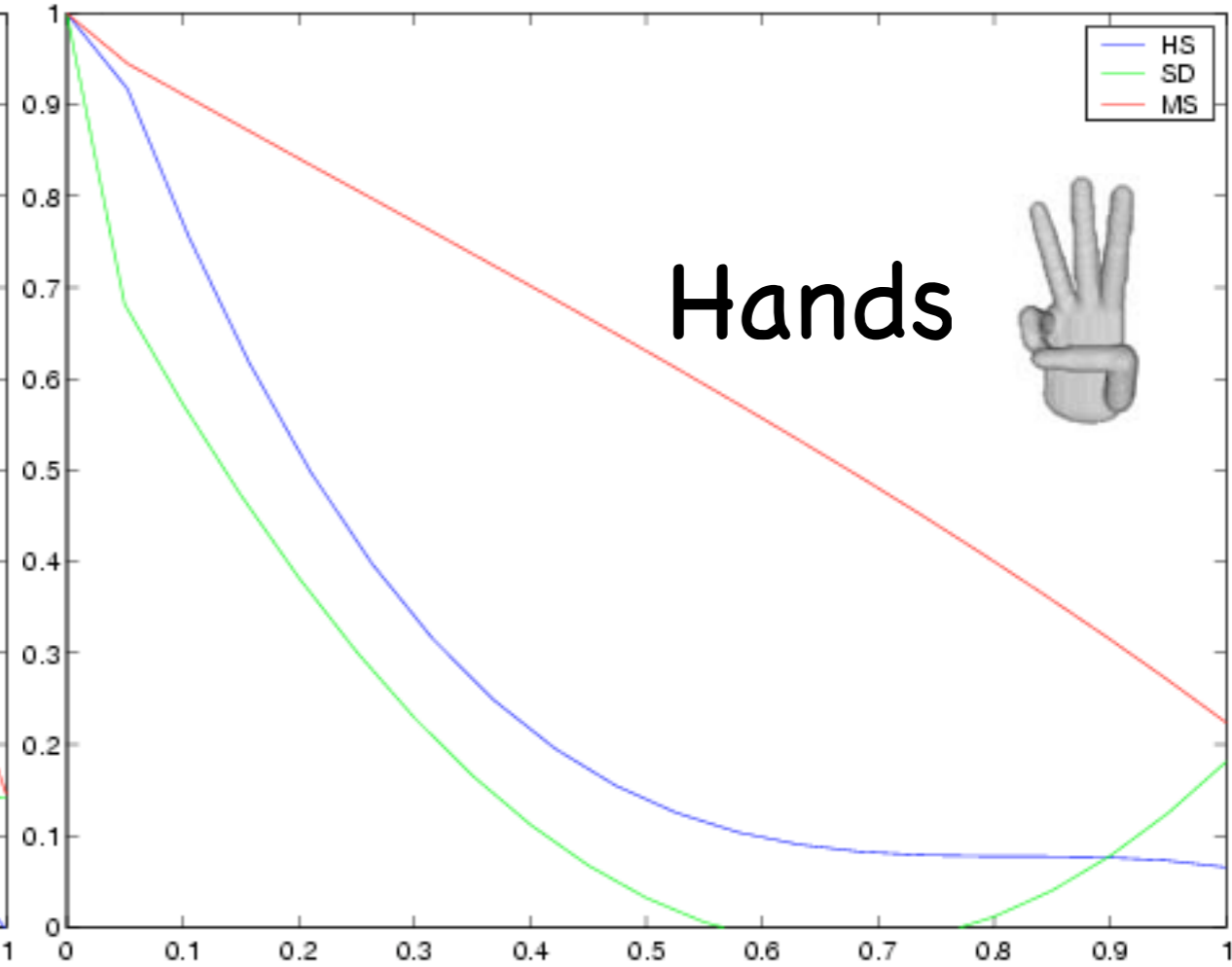
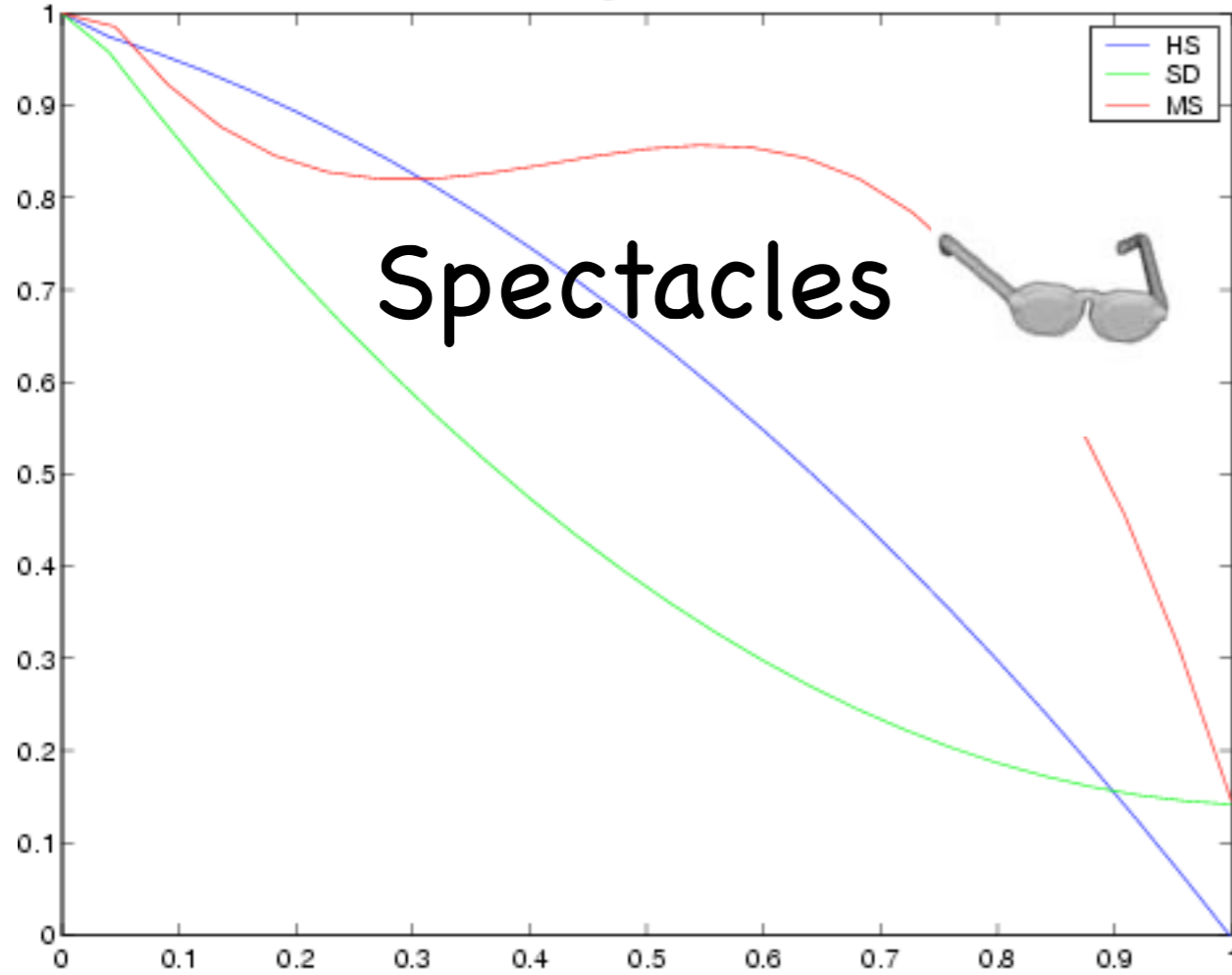
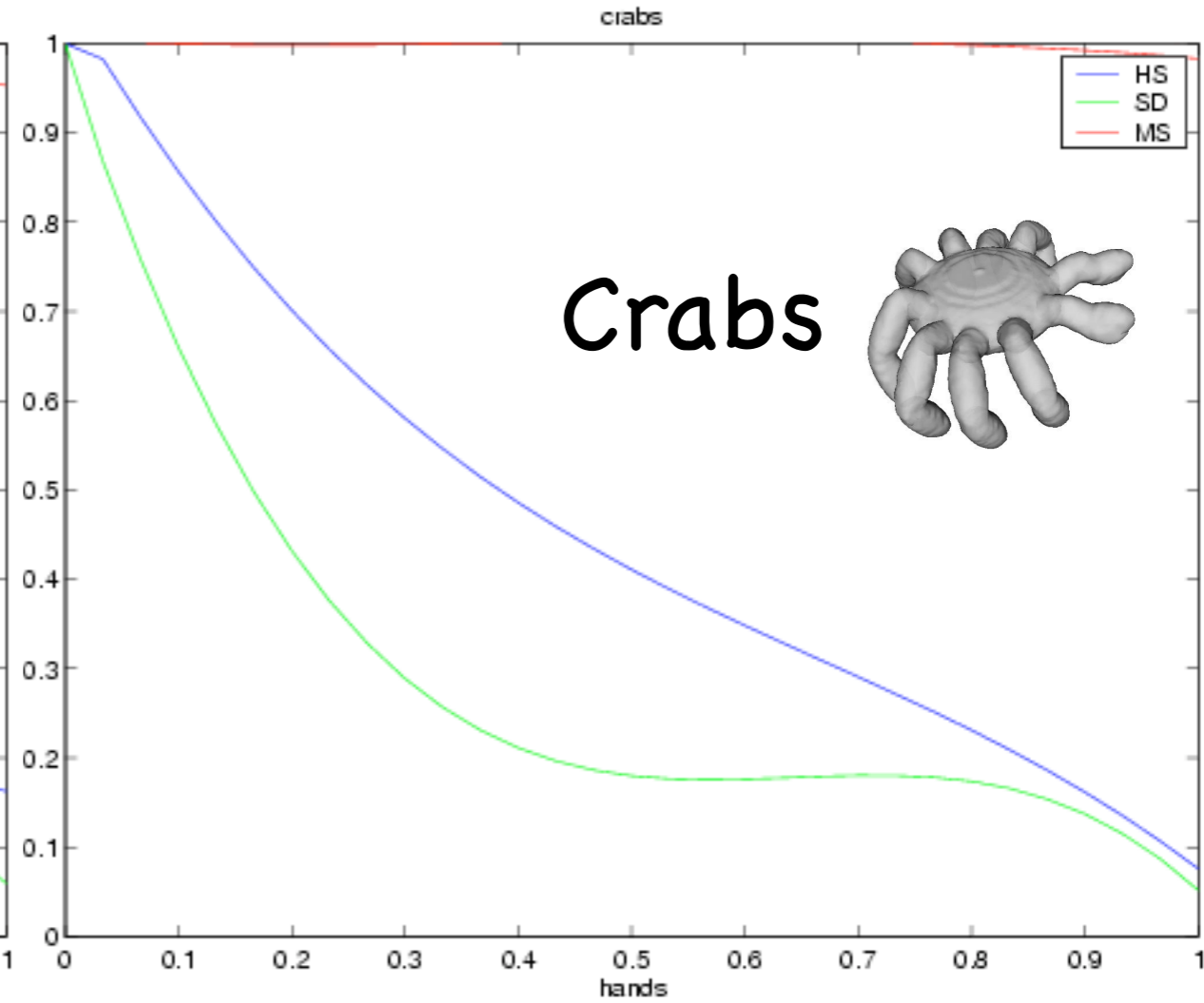
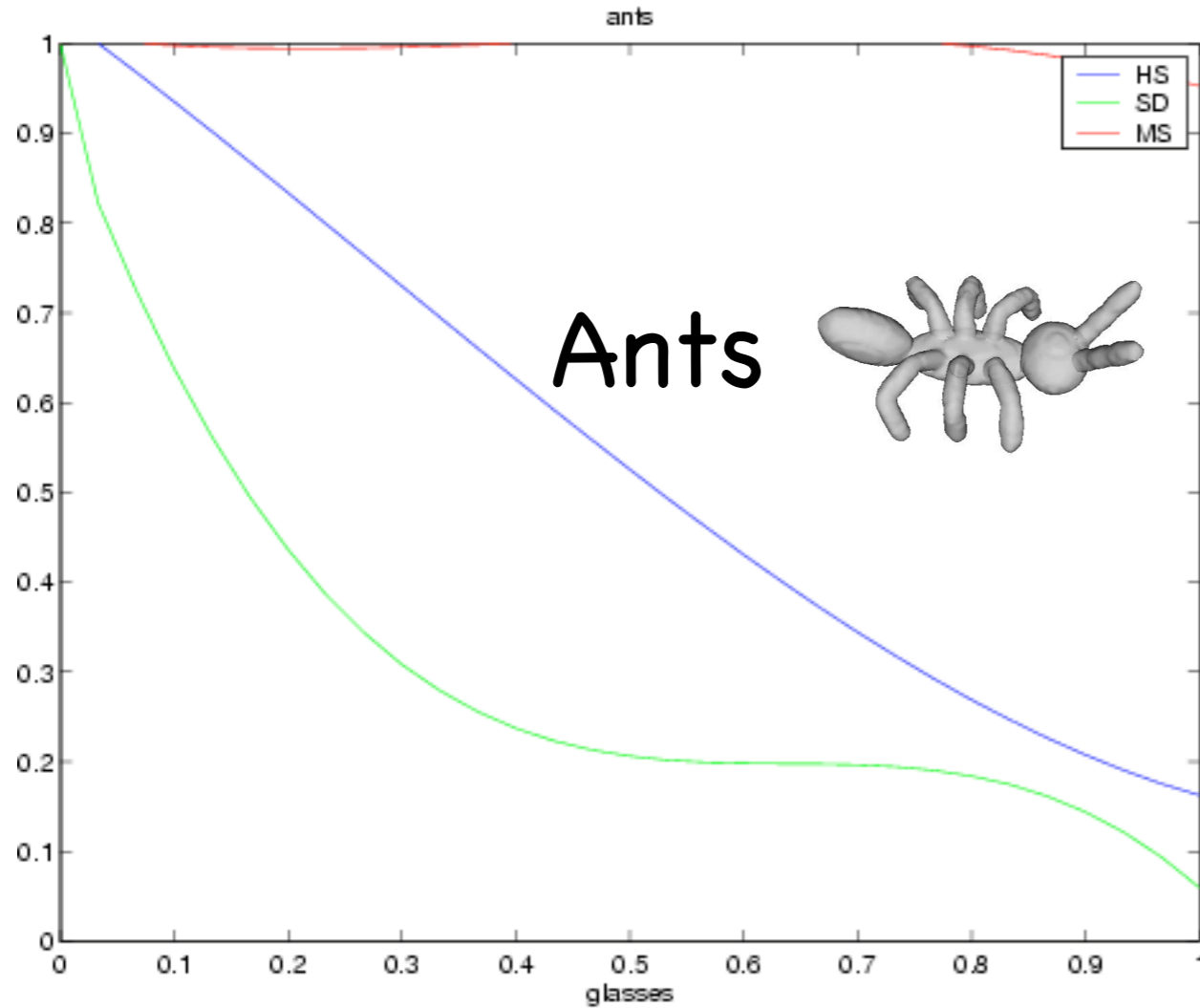
# Medial Surfaces to DAGs

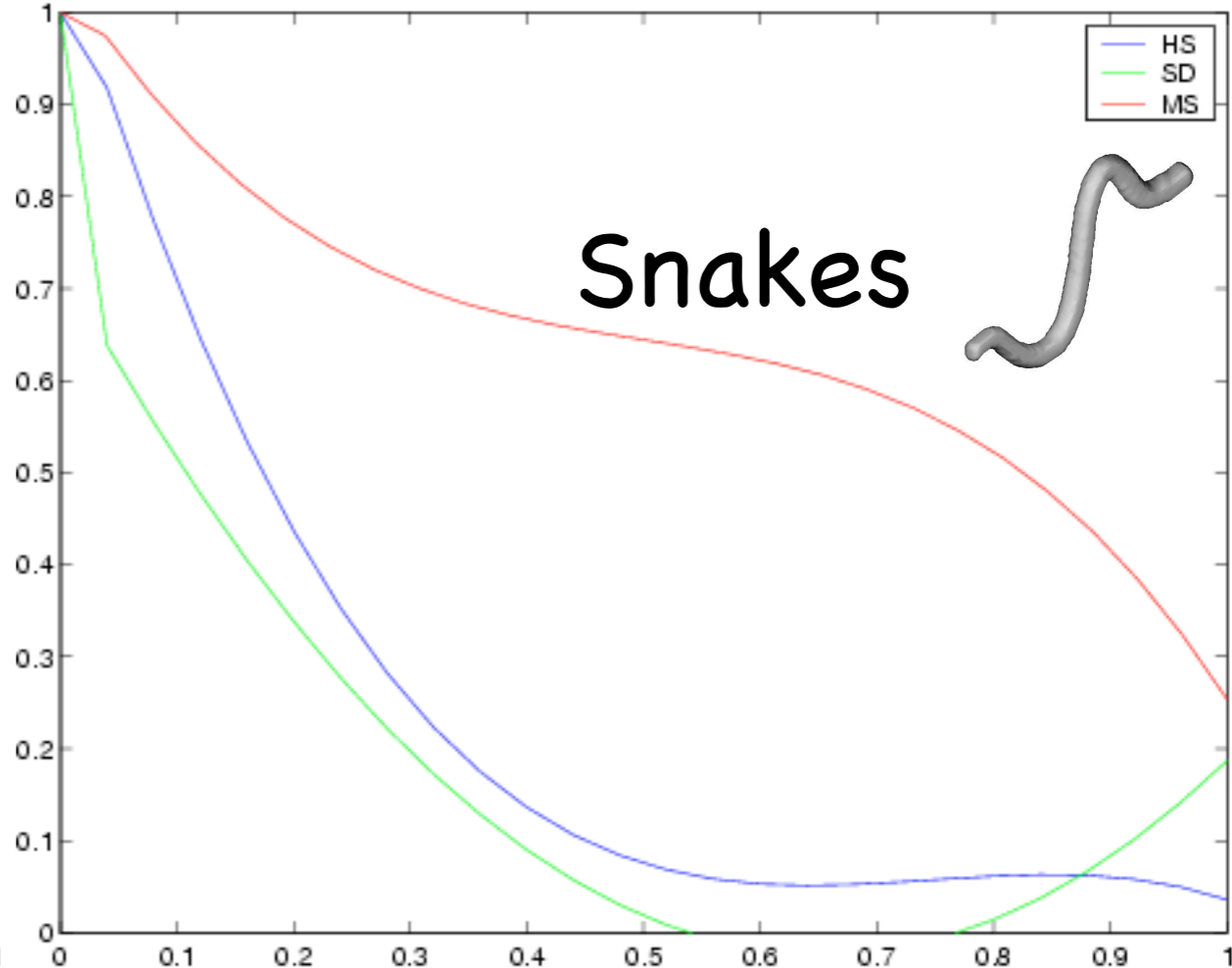
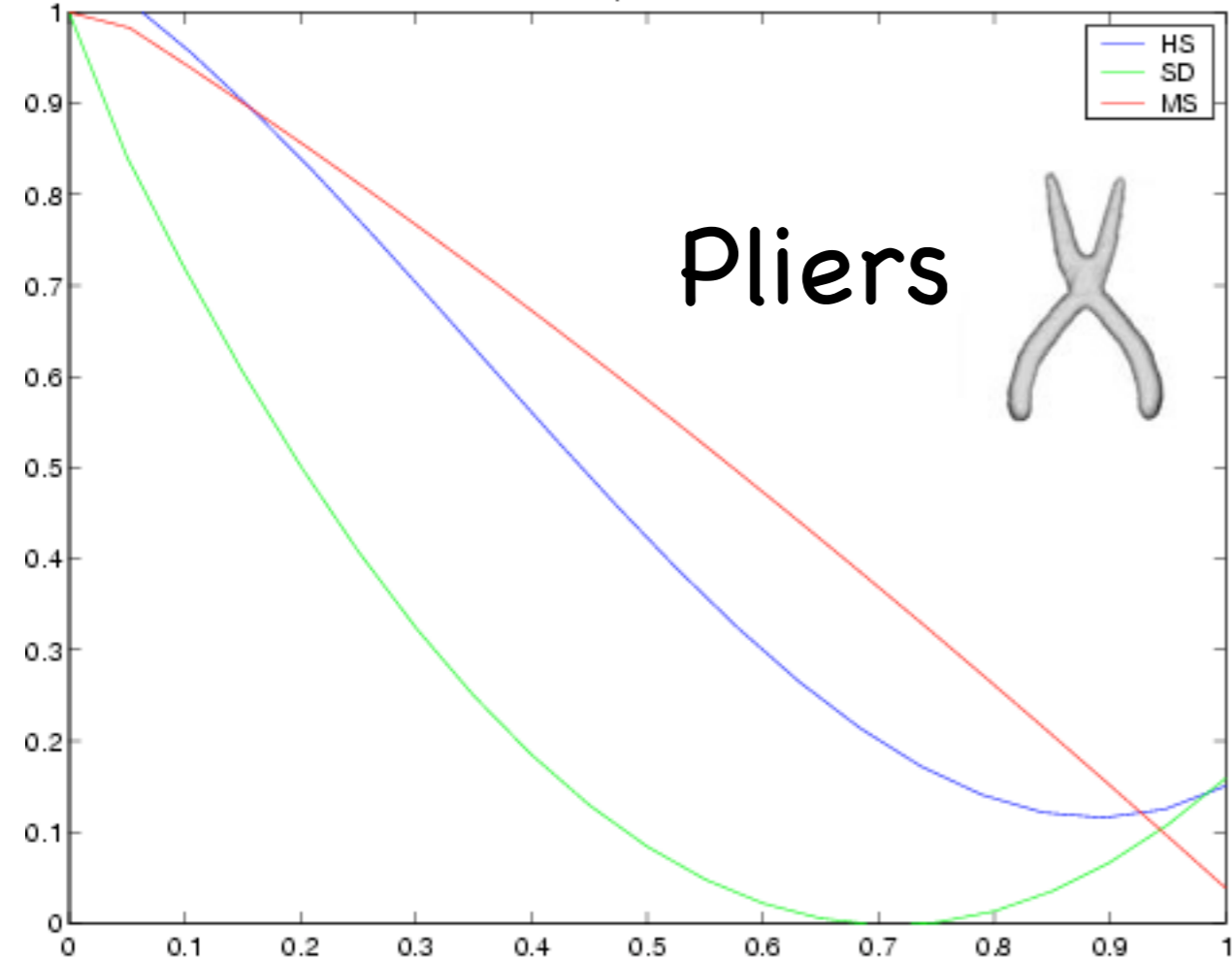
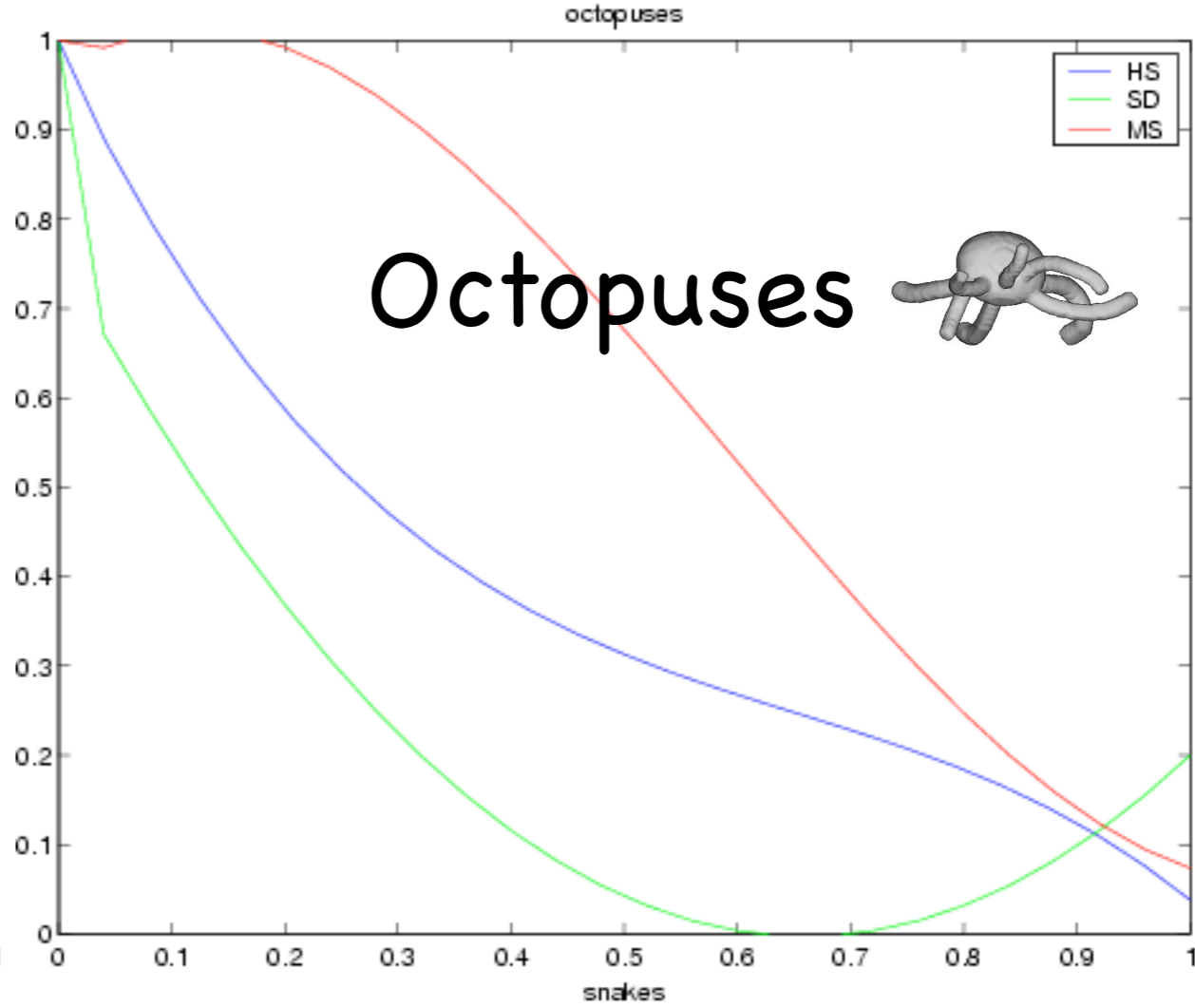
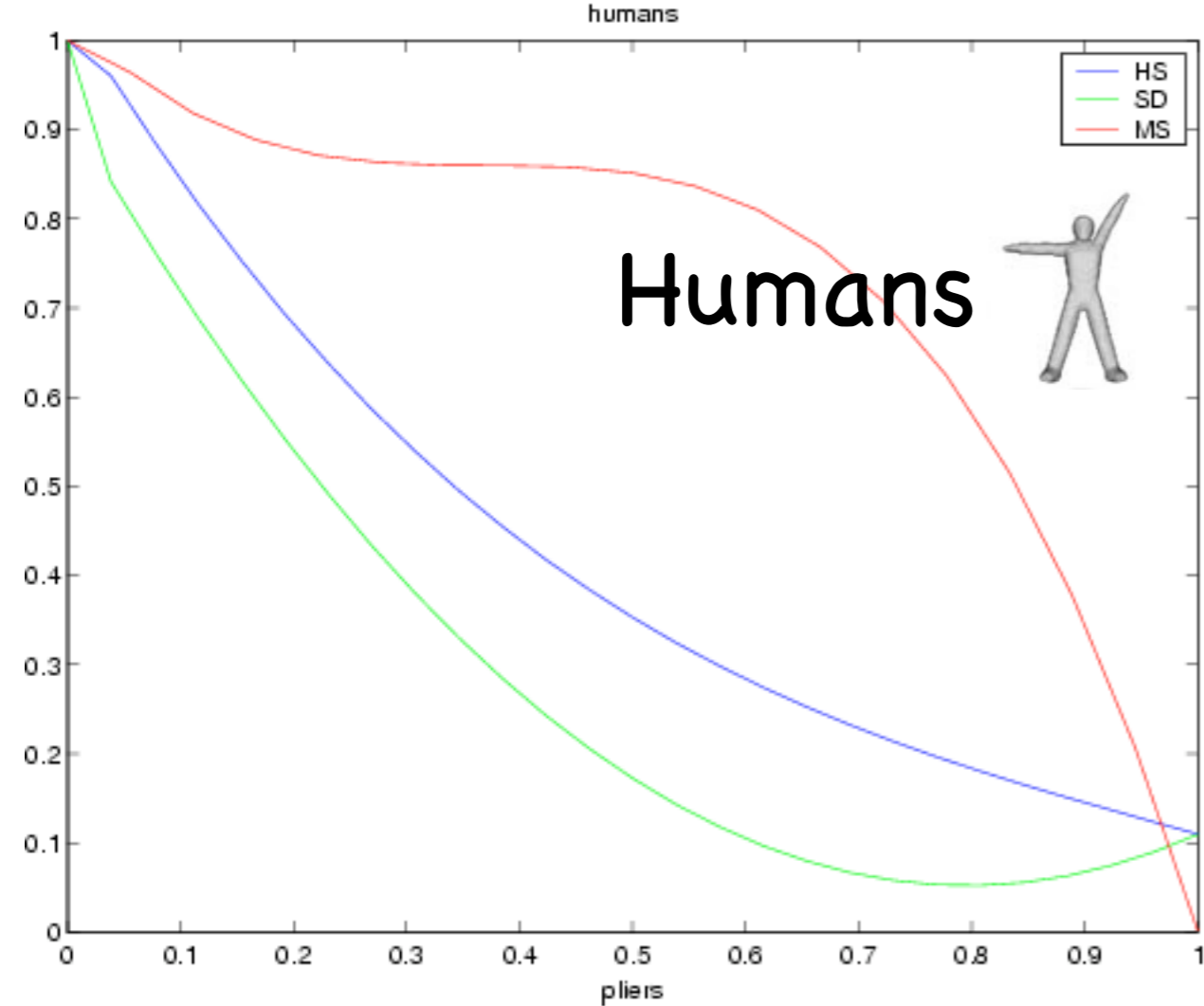


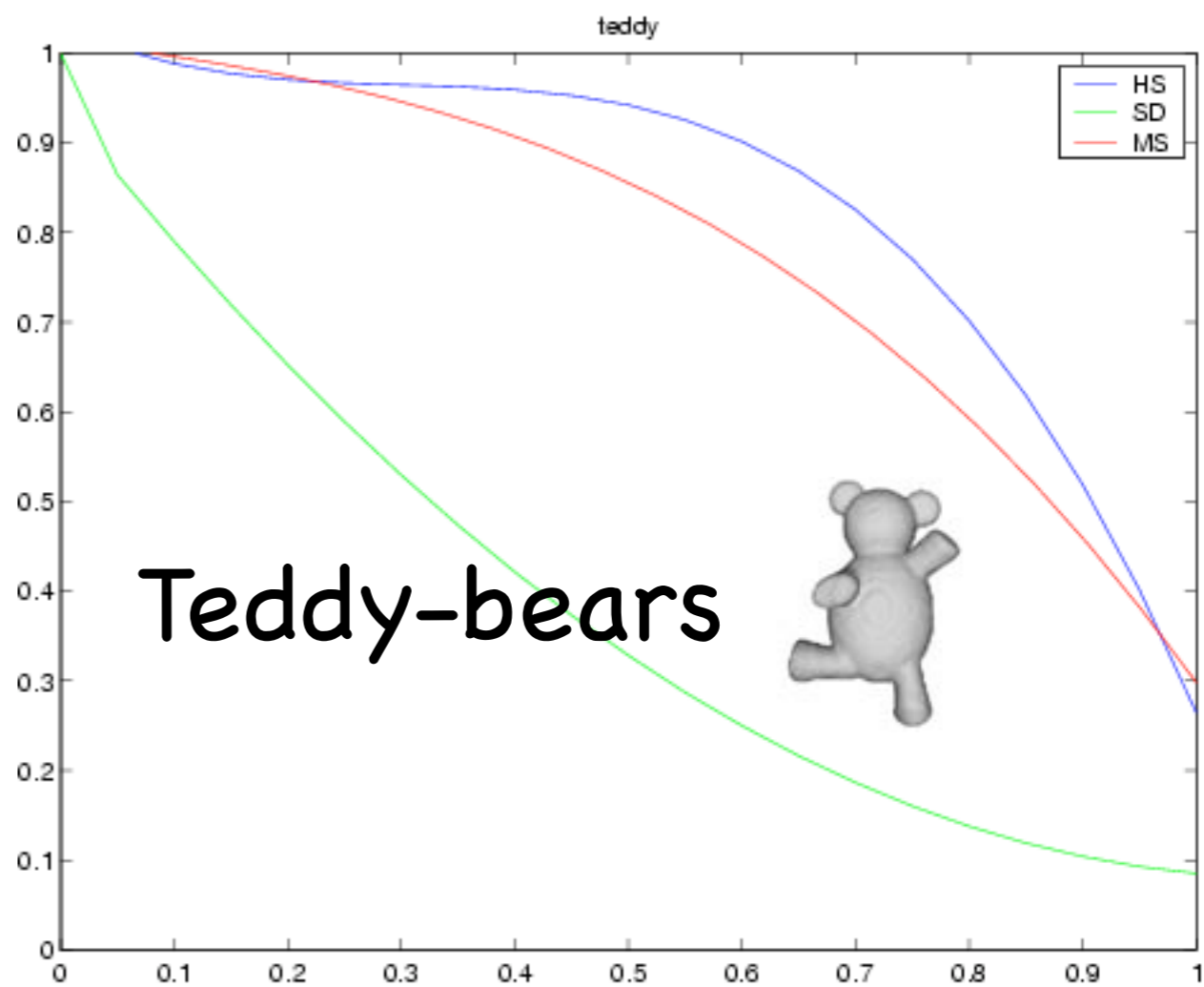
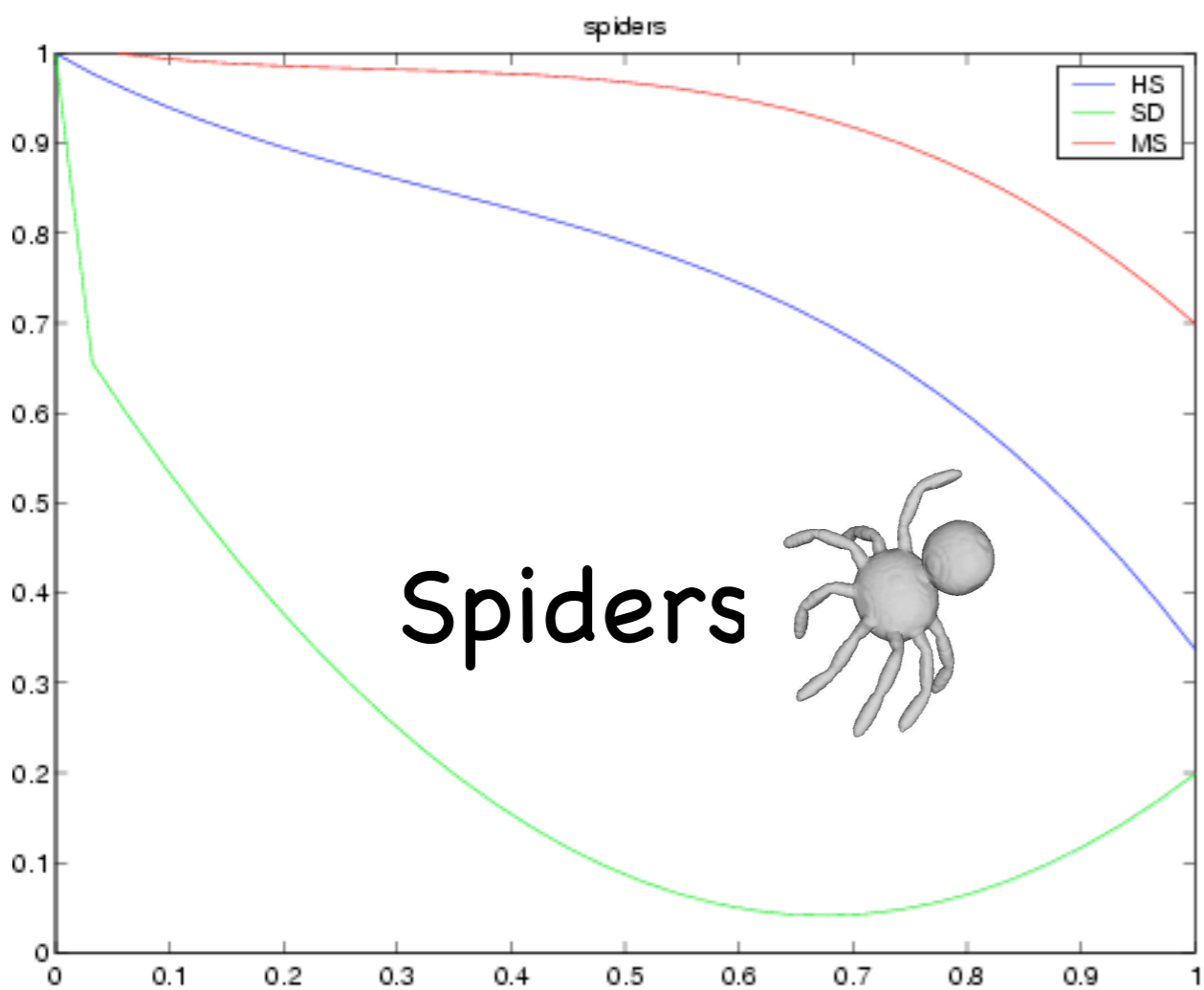
(Malandain, Bertrand,  
Ayache, IJCV'03)

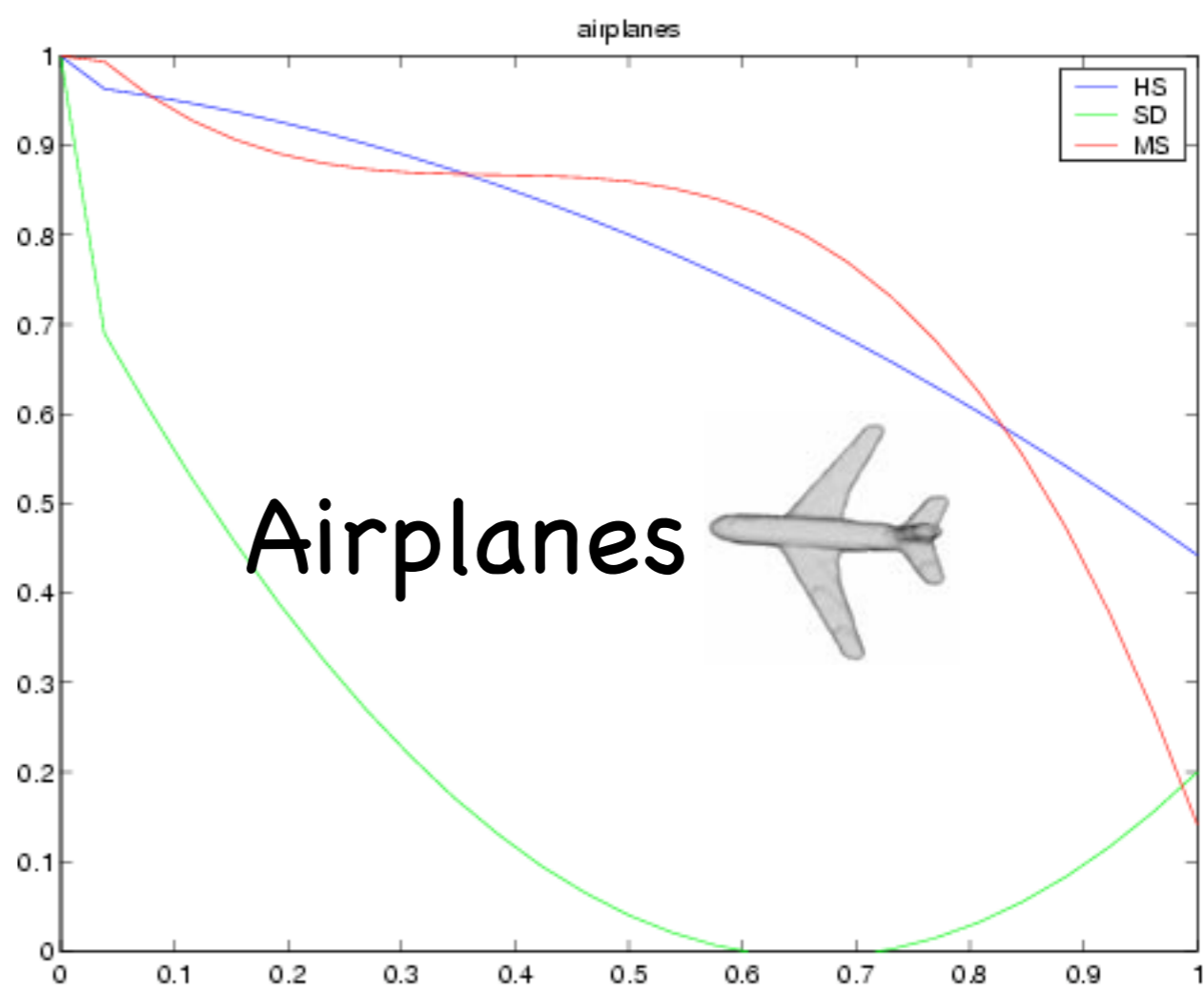
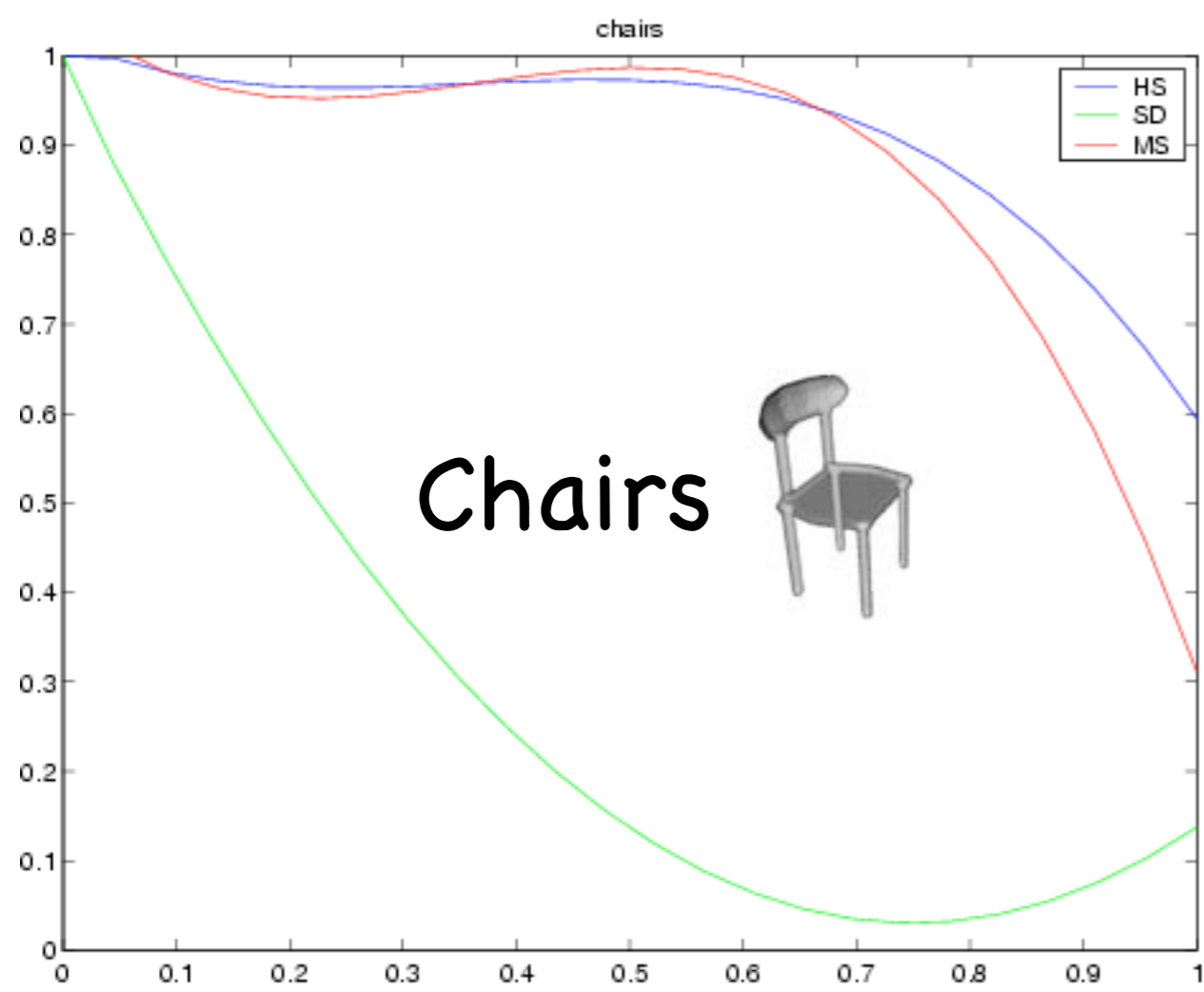
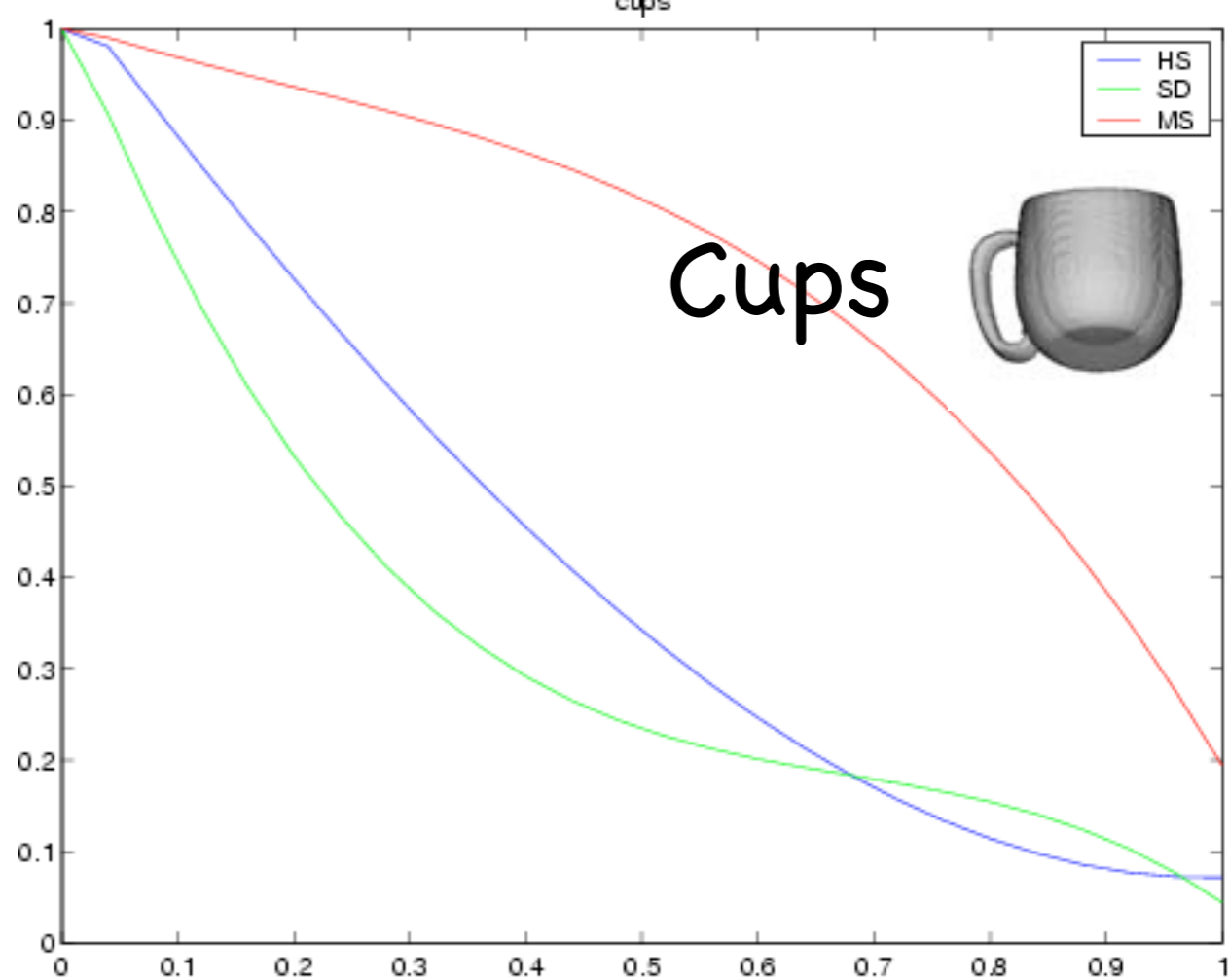
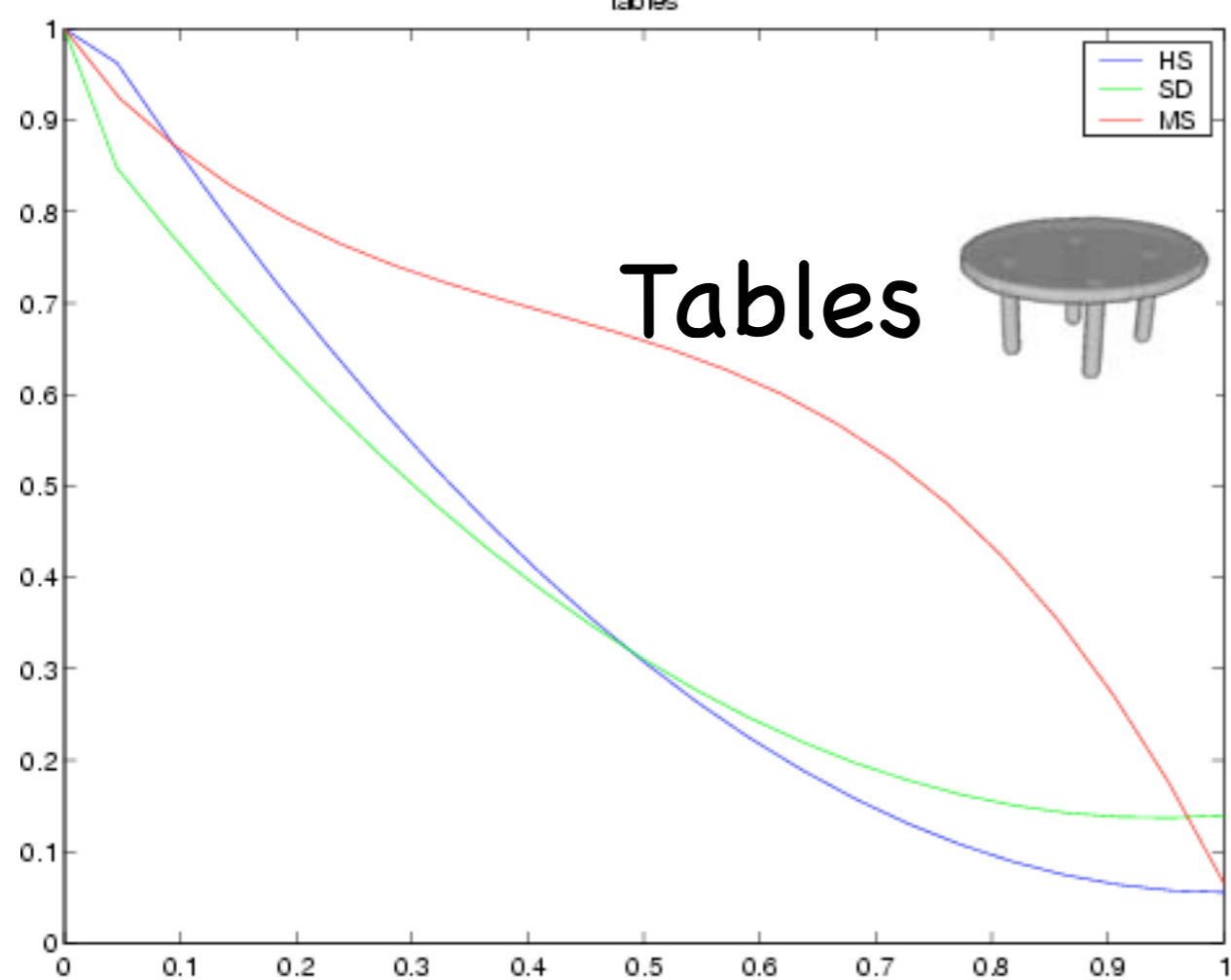
# 3D Object Models: The McGill Shape Benchmark

- 420 models reflecting 18 object classes
- **Severe Articulation:** hands, humans, teddy-bears, eyeglasses, pliers, snakes, crabs, ants, spiders, octopuses
- **Moderate or No Articulation:** planes, birds, chairs, tables, cups, dolphins, four-limbed animals, fish
- **Precision Vs Recall Experiments:** shape distributions of Osada et al. (**SD**), harmonic spheres of Kazhdan et al. (**HS**) and medial surfaces (**MS**).









Summary

# Medial Representations

Mathematics, Algorithms and Applications

Kaleem Siddiqi and Stephen M. Pizer  
Springer (in press, 2006)

- Chapter 1: Pizer, Siddiqi, Yushkevich: "Introduction"
- **PART 1 - MATHEMATICS**
- Chapter 2: Giblin, Kimia: "Local Forms and Transitions of the Medial Axis"
- Chapter 3: Damon: "Geometry and Medial Structure"
- **PART 2 - ALGORITHMS**
- Chapter 4: Siddiqi, Bouix, Shah: "Skeletons Via Shocks of Boundary Evolution"
- Chapter 5: Borgefors, Nystrom, Sanniti di Baja: "Discrete Skeletons from Distance Transforms."



# Medial Representations

Mathematics, Algorithms and Applications

Kaleem Siddiqi and Stephen M. Pizer  
Springer (in press, 2006)

- Chapter 6: Szekely: "Voronoi Skeletons"
- Chapter 7: Amenta and Choi: "Voronoi Methods for 3D Medial Axis Approximation"
- Chapter 8: Pizer et al.: "Synthesis, Deformation and Statistics of 3D Objects Via M-reps"
- **PART 3 - APPLICATIONS**
- Chapter 9: Pizer et al.: "Statistical Applications with Deformable M-Reps"
- Chapter 10: Siddiqi et al: "3D Model Retrieval Using Medial Surfaces"
- Chapter 11: Leymarie, Kimia: "From the Infinitely Large to the Infinitely Small"

# Selected References

- **Bouix, Siddiqi**, "Optics, Mechanics and Hamilton-Jacobi Skeletons" [Advances in Imaging and Electron Physics, 2005]
- **Damon**, "Global Geometry of Regions and Boundaries via Skeletal and Medial Integrals" [preprint, 2003]
- **Dimitrov**, "Flux Invariants for Shape" [M.Sc. thesis, McGill, 2003]
- **Dimitrov, Damon, Siddiqi**, "Flux Invariants for Shape" [CVPR'03]
- **Pelillo, Siddiqi, Zucker**, "Matching Hierarchical Structures Using Association Graphs" [ECCV'98, PAMI'99]

# Selected References

- Sebastian, Klein, Kimia, "Recognition of Shapes By Editing their Shock Graphs" [ICCV'01, PAMI'04]
- Shokoufandeh, Macrini, Dickinson, Siddiqi, Zucker, "Indexing Hierarchical Structures Using Graph Spectra" [CVPR'99, PAMI'05]
- Siddiqi, Bouix, Tannenbaum, Zucker, "Hamilton-Jacobi Skeletons" [ICCV'99, IJCV'02]
- Siddiqi, Shokoufandeh, Dickinson, Zucker, "Shock Graphs and Shape Matching" [ICCV'98, IJCV'99]
- Stolpner, Siddiqi "Revealing Significant Medial Structure in Polyhedral Meshes" [3DPVT'06]